Reconstruction of Loch Lomond Stadial (Younger Dryas) glaciers on Ben More Coigach, NW Scotland, and implications for reconstructing palaeoclimate using small ice masses

Benjamin M. P. Chandler* and Sven Lukas
School of Geography, Queen Mary University of London, Mile End Road, London, E1 4NS
* Corresponding author: b.m.p.chandler@qmul.ac.uk

Abstract

A significant inventory of evidence exists for Loch Lomond Stadial (LLS; ≈Younger Dryas) glaciation in Scotland, with recent work focused on satellite icefields. However, studies of more marginal settings are important for assessing the influence of topoclimatic factors on glacier functioning and, crucially, the impact of these on glacier-derived palaeoclimatic reconstructions. We present systematic assessments of snowblow and avalanching contributions, informed by modern analogues, and test these using the first detailed palaeoglaciological reconstructions of three corrie glaciers on Ben More Coigach, NW Scotland. Based on morphostratigraphic principles, and lithostratigraphic evidence from the region, these have been attributed to the LLS, with the reconstructions yielding an average equilibrium-line altitude (ELA) of 328 ± 16 m. A glacier-derived sea-level equivalent precipitation value of 1903 ± 178 mm a^{-1} is inferred for the LLS, suggesting wetter conditions than currently and contradicting assertions of a more arid LLS climate. Comparison with published palaeoprecipitation estimates indicates Ben More Coigach does not conform to expected regional precipitation gradients. We argue that these discrepancies reflect topographically-enhanced snow accumulation, which lowered the ELA from the 'true' climatic ELA. This highlights the importance of assessing the influence of topoclimatic factors when applying small glaciers in palaeoclimatic reconstructions.

Keywords: Loch Lomond Stadial; NW Scottish Highlands; corrie glaciers; glacier reconstruction; palaeoclimate

Introduction

The clarity and abundance of geomorphological and sedimentological evidence for Loch Lomond Stadial (LLS; ≈Younger Dryas; ~12.9–11.7 ka) glaciation in Scotland has led to the development of a significant body of geomorphological, sedimentological and chronological data pertaining to this event (e.g. Golledge, 2010; Ballantyne, 2012; Bickerdike et al., 2016). This evidence has been employed to produce three-dimensional palaeoglaciological reconstructions and, in turn, to derive palaeoprecipitation estimates (e.g. Ballantyne, 2002, 2007a, b; Benn and Ballantyne, 2005; Lukas and Bradwell, 2010; Finlayson et al., 2011; Boston et al., 2015), which form a crucial component of Quaternary environmental reconstructions: quantitative precipitation estimates cannot be obtained by other proxies. Considerable research effort over the last 10–15 years has markedly advanced our understanding of the extent and dynamics of satellite icefields in Scotland (e.g. Benn and Ballantyne, 2005; Benn and Lukas, 2006; Lukas and Bradwell, 2010; Finlayson et al., 2011; Pearce, 2014; Pearce et al., 2014; Boston et al., 2015), but more marginal settings of (corrie) glaciation have received far less attention (e.g. Ballantyne et al., 2007; Jones et al., 2015; Kirkbride et al., 2015). Although having less extensive and complex geomorphological and sedimentary records, examining sites of potential LLS corrie glaciation is important for assessing the influence of topoclimatic factors such as snowblow (cf. Mitchell, 1996; Carr, 2001; Coleman et al., 2009; Mills et al., 2009, 2012).

In NW Scotland, recent studies have principally focused on (i) reconstructing the dynamics and deglaciation of the Last British-Irish Ice Sheet (e.g. Stoker and Bradwell, 2005; Bradwell et al., 2007, 2008a, b) and (ii) the pattern, timing and dynamics of the Sutherland LLS mountain icefield (e.g. Lukas, 2005a, b; Benn and Lukas, 2006; Lukas and Bradwell, 2010). However, this region contains a number of proposed sites of corrie glaciation that have yet to be the focus of detailed palaeoglaciological studies. Bradwell (2006) highlighted a number of corries as possible sources for LLS glaciers, supporting earlier work by Sissons (1977) and Lawson (1986), but no detailed reconstructions were presented. Thus, there is a need to re-examine these localities using modern approaches to palaeoglaciological reconstruction (e.g. Benn and Hulton, 2010; Boston et al., 2015; Pellitero et al., 2015, 2016). In this contribution, we examine three corries on the Ben More Coigach (BMC) massif, and aim to (i) re-evaluate the geomorphological evidence for glaciation of BMC, (ii) reconstruct the three-dimensional form of inferred ice masses, and (iii) examine the palaeoclimatic significance of the

reconstructed glaciers, in particular taking into account systematic analyses of confounding factors on glacier size and functioning such as snowblow.

Study area and previous work

The study area comprises an area of ~10 km^2 surrounding the multi-summited BMC massif, NW Scotland (Figures 1 and 2; 57^{o}58' – 58^{o}00'N; 5^{o}15' – 5^{o}10'W; British National Grid: NC 074038 to NC 124079). BMC (743 m OD) is located to the west of the Moine Thrust Zone and is composed of Neoproterozoic Torridon Group sandstones. The Torridon Group comprises a thick and remarkably uniform sequence of coarse, red, thick-bedded sandstone with subsidiary layers of pebble conglomerate, which are separated from the underlying Precambrian basement rocks (Lewisian Gneiss complex) by a major unconformity (Goodenough et al., 2009). Further details on the geology of the region can be found elsewhere (e.g. Peach et al., 1907; Johnstone and Mykura, 1989; Goodenough et al., 2009).

Early investigations of the Quaternary glacial history of BMC date back to the 1800s, with Chambers (1853: 233) describing 'a striking collection of hummocks and ridges of detrital matter, with some huge blocks perched on the summits of rocky eminences' in the valley to the north of BMC, which he considered 'true' moraines. The first mapping of the area was conducted by officers of the Geological Survey in the late 19th century (Peach and Horne, 1892) but, with the focus on geology, lacked detailed mapping of glacial features and was restricted to the identification of striae. Charlesworth (1955) identified the massif as a glacier source area in his 'Stage M', which elsewhere approximates several accepted LLS glacial limits (cf. Golledge, 2010; Lukas and Bradwell, 2010). Subsequently, Sissons (1977) mapped sequences of nested moraines in front of three corries on the northern side of the BMC massif and defined glacial limits for three independent LLS corrie glaciers (Figure 2). Occupancy of the three corries during the LLS was also advocated by Lawson (1986, 1995). More recently, this view was supported by Bradwell (2006) based on preliminary investigations of aerial photography and Quaternary geological mapping, although no geomorphological maps or detailed palaeoglaciological reconstructions were presented. In a broader context, recent research efforts in the Coigach area have focused on the extent, dynamics and deglaciation of the Last British-Irish Ice Sheet (e.g. Stoker and Bradwell, 2005; Bradwell et al., 2007, 2008a, b), with well-developed bedforms evident on the southern flank of BMC.

Methods

Geomorphological mapping was conducted using a combination of remote-sensing and field mapping, which is an established procedure in glacial geomorphology (e.g. Hubbard and Glasser, 2005; Boston, 2012; Darvill et al., 2014; Pearce et al., 2014; Chandler et al., 2016; Ewertowski et al., 2016). Mapping focused on identifying landforms that could be employed to reconstruct discrete ice masses. Three remote-sensing datasets were employed in this study: (i) the NEXTMap Britain topographic dataset (Intermap Technologies, 2007); (ii) panchromatic aerial photographs from the All Scotland Survey at ~1: 24,000 scale; and (iii) orthorectified digital colour aerial photographs with a resolution of 0.25 m GSD (Ground Sampled Distance). The final geomorphological map is predominantly based on field mapping conducted on topographic base maps at a scale of 1: 10,000, with remote-sensing used to ensure accurate representation of the shape, size and orientation of features; in particular, moraines were mapped on acetates overlying panchromatic aerial photograph stereopairs (cf. Benn and Ballantyne, 2005; Lukas and Lukas, 2006; Boston, 2012). Acetates were scanned and georectified using the approach outlined by Lukas and Lukas (2006), with the mapping assimilated broadly following the workflow of Boston (2012). Methods relating to glacier reconstruction, equilibrium-line altitude estimation and palaeoclimate calculations are detailed in the appropriate sections.

Results

Description of geomorphological evidence

The study area, centred on the valley between BMC [NC 094042] and Beinn an Eoin [NC 104064], contains an abundance of well-preserved glacial landforms found in close association with three corries on the northern side of the BMC massif (Figure 3). These features manifest in the form of a series of conspicuous nested moraines with broadly arcuate planforms, and these are found in association with spreads of glacially-transported boulders. Beyond the limits of the outermost moraines, the valley is characterised by bedrock protuberances, some of which are ice-moulded [e.g. NC 097059], through a blanket peat cover. Additionally, striae are evident in a few places within the valley (Figure 3). Further downvalley towards Loch Lurgainn, beyond the mapped limits, roches moutonneés are also evident [NC 138054]. The abundance and clarity of the glacial landforms found in close

association with the corries of BMC warrant further detailed investigation, and these are described below.

Cadh' a' Mhoraire

On the valley floor in front of Cadh' a' Mhoraire lies a striking suite of moraines spanning ~210–265 m (Figures 3 and 4). The boulder-strewn outermost moraine is particularly prominent, reaching a maximum height of ~6 m on its distal side and ~4 m on its ice-proximal side, and forms the southeastern margin of the lochan. The moraine has an undulating crestline, a length of ~970 m and is broadly arcuate in planform, albeit in detail somewhat irregular. It is flat-topped and displays an asymmetric cross profile, with a steeper distal (~34°) and a gentler ice-proximal slope (~28°). On its eastern end, the moraine curves around to the SW and the ridge crestline can be traced to a series of small, low elevation (~2 m high) mounds that trend back towards the corrie. Nested within the outermost moraine are a series of moraine fragments (n = 121; surface area = 64–5,652 m^2), which are littered with glacially-transported boulders of local lithology (Torridonian sandstone). The individual ridges and mounds form a series of inset arcuate chains of moraines, and they display similar morphological characteristics to the outermost moraine. These moraines range in height from 2–4 m on their proximal sides and 3–6 m on their distal sides, though infilling with glacial debris and peat has frequently reduced their apparent height. To the south of the innermost moraine in this assemblage, accumulations of glacially-transported boulders are evident, all of local lithology. Near the eastern wall of the corrie [NC 110050], some of the boulders form a distinctive boulder dispersal train, extending down from ~340 m OD to ~270 m OD, which coincides with the moraine crestlines on the valley floor below. Further up the corrie, near the eastern wall, lie a series of approximately-parallel linear ridges ranging in length from ~20–65 m. Aside from the geomorphological features mentioned, this corrie is characterised by the presence of a number of prominent gullies incised into the backwall, with a small debris cone [NC 105050] emanating from the northernmost of these gullies.

Sgùrr an Fhidleir

A series of moraine ridges and mounds is identifiable to the northeast/east of Sgùrr an Fhidleir [NC 094054; 705 m OD], though the suite is less expansive than that in the neighbouring corries (Figure 3). The outermost moraine comprises four discrete ridges and a

few mounds, which can be traced along the southwestern edge of Lochan Tuath to form a broadly arcuate feature. The individual moraine ridges have lengths ranging between ~45 m and ~240 m, with maximum heights of ~4 m on the distal and ~2 m on the proximal flank. The outermost moraine displays an asymmetric cross-profile, with a steeper distal (~31°) and gentler ice-proximal slope (~21°). At the northwestern end [NC 098057], this feature can be traced around to mounds that trend towards the corrie in a southeasterly direction. Nested within the outermost moraine are a number of discrete mounds and ridges (n = 43; surface area = 82–1,617 m^2), displaying similar asymmetric cross-sections; they vary in height from 2–4 m on their distal and 1–2 m on their ice-proximal side. Additionally, there is a spread of glacially-transported boulders situated inside the moraine assemblage.

An Clù-nead

On the valley floor to the N/NNW of Sgùrr an Fhidleir, in the vicinity of An Clù-nead, is an assemblage of closely-spaced moraine mounds and ridges (n = 134) that spans ~100–180 m. The outer limit of this suite comprises a series of mounds and ridges that form an arcuate chain ~1.1 km in length, with individual ridges reaching maximum lengths of ~205 m. Mounds extend across the valley floor, descending from ~320 m OD [NC 093059] to ~250 m OD [NC 095064], arcing around to the NW [NC 096061] and W [NC 092064] towards a small debris cone. At its eastern extent, the moraine assemblage abuts an outcrop of ice-moulded bedrock (Figure 3). Similar to features in front of the neighbouring corries, the moraine is flat-topped, exhibiting an asymmetric cross-section with particularly steep distal (34°) and gentler ice-proximal faces (22°). It reaches a maximum height of 7 m on its distal side and 3 m on its ice-proximal side. Inset within the outer moraine are numerous ridges and mounds of varying size (surface area = 44–2,232 m^2). The crestlines of the discrete mounds and ridges can be traced to form a series of long, inset, arcuate chains. These ridges display similar morphological characteristics to the outermost moraine, and reach heights of ~2–4 m. Associated with the moraines are a number of spreads of glacially-transported boulders (maximum *a*-axes ~5 m), all of local lithology. Aside from these features, gullies incised into the plateau rim and corrie backwall are also evident, similar to those identified in the Cadh' a' Mhoraire corrie.

Periglacial and paraglacial features

To the north of An Clù-nead, the valley flanks are characterised by 'mature' talus, with the eastern flank exhibiting a fairly uniform talus accumulation (talus sheet) at the slope foot. This talus sheet is completely vegetated and displays minimal evidence of rockfall debris onto the vegetation cover. Moreover, limited talus reworking is evident on the eastern flank. Conversely, the western flank of the valley exhibits evidence of talus remobilisation by debris flows. The western slopes do, however, bear some resemblance to those on the eastern flank: they are completely vegetated and show no evidence of fresh rockfall debris accumulation. A notable feature of the western valley side is the clear contrast between slope features within the confines of the moraines and those beyond the outermost moraine: slopes within the limits are characterised by small debris flow deposits and debris cones, whereas slopes beyond the outer moraine are characterised by thick, mature talus and larger debris cones.

On the higher ground surrounding BMC and Sgùrr an Fhidleir, the plateau is dominated by aeolian features, including turf-banked terraces and aeolian sand deposits. Higher parts of the undulating plateau support tor-like outcrops, which show signs of superficial frost-weathering (microgelifraction), and widespread coverage of wind-scoured frost-weathered regolith (deflation surfaces). Deflation surfaces and aeolian sand deposits cover the majority of the ground above 550 m OD (Chandler, 2013). This assemblage of periglacial features is not included on the map or discussed further in this contribution for reasons of clarity, with these characteristic features of Torridonian sandstone plateaux considered elsewhere (cf. Ballantyne, 1995). As mentioned in the previous sections, a number of hitherto-unreported prominent gullies are evident in the corrie headwalls, and these features appear along the NE edge of the BMC massif (Figure 3) where they are deeply incised into the plateau rim. These gullies have widths of 28–110 m (average ~60 m) and depths of 30–109 m (average ~68 m) at the plateau edge. They occur predominantly in areas that are upvalley of the moraines described in detail above and just downslope of prominent plateau areas. Conversely, gullies are largely absent from steeply-dipping areas of the massif that do not show this association.

Interpretation of the geomorphology

The glacial geomorphology mapped and described provides clear evidence for three distinct glacial limits, demarcated by the outermost moraines. The three moraine assemblages and the features evident inside them contrast with the landform associations beyond the outermost moraine (Figure 5). Outside the corrie limits, the valley is characterised by protuberances of

bedrock, glacial erosional features, blanket peat cover and a notable absence of glacial depositional features. Conversely, the corries are associated with suites of conspicuous, inset moraines and spreads of glacially-transported boulders, which occasionally align to form dispersal trains. Moreover, slopes within the limits of the moraine assemblages are characterised by limited debris cover at the foot of the slopes, whilst the flanks of the valley beyond the limits of the An Clù-nead moraines are characterised by mature talus. The contrasts in slope features are most evident on the western flank of the valley where debris accumulations grade from small debris flow deposits and debris cones inside the limit of the outermost moraine to mature talus outside the limit. The lack of rockfall debris on the vegetated talus slopes and the occurrence of debris flow deposits on the slopes suggest that erosion has replaced accumulation as the dominant mode of geomorphological activity on the talus slopes (cf. Ballantyne and Harris, 1994; Hinchcliffe and Ballantyne, 2009). On the basis of the contrasts between landform associations either side of the outermost moraines, limits for three locally-nourished palaeoglaciers that existed penecontemporaneously are identified. The relationship between the prominent gullies incised into the plateau rim and the glacial depositional features downvalley implies a glaciologically-significant link that will be further explored in the context of the palaeoglaciological reconstruction.

Age of the palaeoglaciers

Constraining the age of the palaeoglaciers is crucial to derive meaningful palaeoglaciological and palaeoclimatic variables. However, obtaining 'absolute' chronological control has not been possible within the constraints of this research. Consequently, it has not been possible to quantitatively constrain the age of these three palaeo-ice masses. Nonetheless, converging strands of morphostratigraphic evidence (cf. Lukas, 2006; Boston et al., 2015, and references therein) from the study area, and lithostratigraphic evidence from the wider region, permit the age of the palaeoglaciers to be inferred with some confidence.

Conspicuous, nested moraines within the study area are considered indicative of LLS glacial limits by analogy with features elsewhere (e.g. Ballantyne, 1989; Benn et al., 1992; Ballantyne et al., 2007; Bendle and Glasser, 2012; Kirkbride et al., 2015), with subdued moraines commonly occurring beyond the limits of LLS maximum extent (cf. Sissons, 1976; Robinson and Ballantyne, 1979; Ballantyne, 1988; Brown, 1993; Benn, 1997; Bennett, 1999; Lukas, 2006). Moreover, the BMC moraines exhibit morphological characteristics closely

resembling those identified on Hoy, Orkney Islands (Ballantyne et al., 2007). These moraines have yielded ^{10}Be exposure ages that demonstrate the Hoy corrie glaciers existed during the LLS. Furthermore, the presence of numerous glacially transported boulders has been observed to coincide with former LLS glacier limits elsewhere in Upland Britain (e.g. Sissons, 1977; Gray, 1982; Thorp, 1986; Hughes, 2002; Ballantyne, 2007a). Thus, the occurrence of boulder spreads within the defined BMC glacial limits provides further evidence suggestive of a LLS age. Marked contrasts also exist between slope features inside and outside the proposed glacial limits: slopes inside the limits are characterised by small debris flow deposits and debris cones, whilst slopes beyond the outermost moraines are covered by mature talus. Previous research has demonstrated that the LLS represents the last period of intense periglacial activity affecting Upland Britain (e.g. Ballantyne and Harris, 1994); thus, extensive mature talus would have accumulated on non-glaciated slopes that were affected by enhanced frost weathering during the LLS (Ballantyne and Eckford, 1984; Ballantyne, 1991). This strand of evidence, therefore, is consistent with a LLS age for the BMC palaeoglaciers. Similar morphostratigraphic relationships to those at BMC have been identified at Arkle, NW Scotland, and the Arkle corrie glacier complex has been dated to the LLS through analogy with a nearby penecontemporaneous glacial limit that has independent age control (Lukas, 2006; Lukas and Bradwell, 2010).

Aside from the geomorphological evidence, a number of dates from the region provide supporting evidence. Investigations of Loch Sionascaig (~9 km to the NNE) and Cam Loch (~15 km to the NE) have yielded complete and unconformable Lateglacial tripartite sequences (Pennington et al., 1972; Pennington, 1977). Dates of 11,638–9,213 and 11,412–9181 cal a BP from Cam Loch [calibrated to 2σ using CALIB 7.1; Stuiver et al. (2016)], closely resemble the end of the LLS as recorded elsewhere in Scotland (cf. Brooks and Birks, 2000a). A subsequent return to organic sedimentation is evident, dated to 10,496–9,355 cal a BP at Cam Loch and 9,249–8,392 cal a BP at Loch Sionascaig. Thus, the lithostratigraphic evidence and radiocarbon dates imply that the Coigach region experienced localised glaciation during the latter part of the Lateglacial. Based on this evidence, together with the geomorphological evidence, we attribute the BMC palaeoglaciers to the LLS, subject to independent chronological control.

Palaeoglaciological reconstruction

The geomorphological evidence allows empirically-based, three-dimensional representations of three independent LLS corrie glaciers to be produced, with the termini of the palaeoglaciers marked by moraines at ~270 m OD (Cadh' a' Mhoraire and Sgùrr an Fhidleir glaciers) and ~250 m OD (An Clù-nead glacier). Owing to an absence of geomorphological evidence constraining the upper surface of the glaciers, a two-dimensional glacier surface profile model was employed; specifically, the 'perfectly plastic' profile model of Benn and Hulton (2010). For modelling the BMC glaciers, an initial basal shear stress of 50 kPa was employed, though lower basal shear stress values (30–50 kPa) were necessary to satisfy the geomorphological evidence at the snouts. The shear stresses were increased as the topographic gradient steepened (Benn and Hulton, 2010; Boston et al., 2015). With no geomorphological evidence in the upper parts of the corries, two scenarios were used: (i) a scenario in which the glacier was forced to intercept the corrie backwall (i.e. shear stress = 0 kPa on the plateau) (Figures 6A–C); and (ii) a scenario where no boundary conditions were imposed, other than the empirical evidence for surface gradient at the snout (Figures 6D–F). The latter scenario, where the glacier surface profile was extrapolated using finite basal shear stresses, resulted in very thin, steep glaciers on the backwall and ice on the plateau surfaces above the corries, which continues to rise in elevation. These represent issues with the implementation of the model in areas with plateau surfaces and/or a steep backwall. In the case of the backwall, calculated glacier thicknesses will always be finite as the model is based on the assumption of a constant basal stress; thus, the glacier surface cannot intercept the backwall (Benn and Hulton, 2010). The upper limits of the corrie glaciers are, therefore, likely to be represented by the sharp inflections in the glacier surface profiles. Nevertheless, the presence of cold-based ice/snowfields on the plateau surfaces above the corrie backwalls cannot be ruled out. Indeed, we argue that the existence of deeply-incised gullies eroded into the corrie backwalls and their association with flat expanses of the massif (Figure 3) provides geomorphological evidence for the presence of cold-based ice or snowfields on the plateau.

In view of the uncertainty over the existence and extent of any cold-based ice, we reconstruct three independent corrie glaciers on BMC (Figure 7). The three-dimensional form of the glaciers was determined using well-established procedures: ice surface contours were manually drawn at 10 m intervals to depict thickness, with their position estimated using topographic base maps and the surface profile modelling results (cf. Boston et al., 2015). At their maximum extent, the respective palaeoglaciers had surface areas of 0.59 km^2 (Cadh' a' Mhoraire), 0.30 km^2 (Sgùrr an Fhidleir) and 0.36 km^2 (An Clù-nead).

341

342 ***Palaeoclimatic reconstruction***

343

344 Equilibrium line altitudes (ELAs) represent the altitude on a glacier where net accumulation
345 and net ablation are equal and, therefore, a sensitive link between glaciers and climate that
346 can be utilised to derive palaeoclimatic variables (e.g. Bakke et al., 2005a, b; Carr et al.,
347 2010; Lukas and Bradwell, 2010; Boston et al., 2015). When computing palaeo-ELAs, it is
348 assumed the reconstructed glacier was under steady-state conditions whilst at its maximum,
349 though this is notional (cf. Boston et al., 2015). Various approaches can be employed to
350 retrodict ELAs for reconstructed ice masses (cf. Meierding, 1982, Benn et al., 2005), though
351 the palaeo-ELAs of LLS glaciers in Scotland are typically calculated using the area-weighted
352 mean altitude (AMWA; Sissons, 1974), accumulation area ratio (AAR; Porter, 1975; Torsnes
353 et al., 1993; Benn and Lehmkuhl, 2000) and area-altitude balance ratio (AABR; Furbish and
354 Andews, 1984; Benn and Gemmell, 1997; Osmaston, 2005) methods. The AABR is widely
355 assessed as the most reliable approach in approximating true climatic ELAs, and overcomes
356 the shortcomings associated with the other approaches by incorporating both glacier
357 hypsometry and variable mass balance gradients in ELA calculations (cf. Osmaston, 2005;
358 Benn and Ballantyne, 2005; Benn et al., 2005; Rea, 2009). AABR methods utilise an
359 assumed balance ratio (BR), with previous Scottish palaeoglaciological studies employing
360 BR values of 1.67, 1.8 and 2.0 to LLS glaciers (e.g. Ballantyne, 2002; Benn and Ballantyne,
361 2005; Lukas and Bradwell, 2010; Finlayson et al., 2011). More recent studies (e.g. Boston et
362 al., 2015; Boston and Lukas, 2016) have used a BR of 1.91 ± 0.81 (± is one standard
363 deviation), which is considered representative of modern mid-latitude maritime glaciers (Rea,
364 2009).

365

366 ELAs for the three BMC corrie glaciers (Table 1) have been generated using a recently
367 published ArcGIS toolbox (Pellitero et al., 2015). This GIS tool utilises a Digital Elevation
368 Model (DEM) of the glacier surface, generated from the ice surface contours, to calculate the
369 ELA. Using a BR value of 1.91 ± 0.81 (ELA3; Table 1) yields ELAs of 345 ± 14 m (Cadh' a'
370 Mhoraire), 335 ± 13 m (Sgùrr an Fhidleir) and 305 ± 11 m (An Clù-nead) for the respective
371 palaeoglaciers. In line with previous studies, we employ the average ELA calculated using a
372 BR of 1.91 ± 0.81 (328 ± 16 m) for subsequent palaeoclimatic calculations. It should be
373 noted that the palaeoglaciological reconstructions utilised to derive the ELAs represent
374 minimum ice coverage, and that any contribution to mass balance from plateau-based ice

would raise the ELAs and, conversely, lower subsequent palaeoprecipitation estimates (cf. Finlayson, 2006).

Palaeoglaciological reconstructions, including previous Scottish studies (e.g. Benn and Ballantyne, 2005; Finlayson, 2006; Lukas and Bradwell, 2010), have employed a nonlinear relationship between temperature and annual precipitation, derived from a global dataset of modern glaciers, to provide estimates of palaeoprecipitation at the ELA (Ohmura et al., 1992) and gain insights into former palaeoclimatic conditions:

$$P = 9T_a^2 + 296T_a + 645 \qquad (1)$$

where P is the sum of winter accumulation and summer precipitation at the ELA (mm a^{-1}) (water equivalent), and T_a is the mean ablation season temperature at the ELA (°C). However, there are discrepancies between precipitation values derived using this approach (e.g. Benn and Ballantyne, 2005; Lukas and Bradwell, 2010) and general circulation models (e.g. Björck et al., 2002; Jost et al., 2005), with the latter implying a much drier climate. Golledge et al. (2010) have argued that the application of a global dataset to a palaeoglaciological question local to Scotland neglects the influence of seasonality upon LLS ice masses and may, therefore, result in overestimation of palaeoprecipitation. Indeed, the Ohmura et al. (1992) dataset has specific issues such as the inclusion of data from Austfonna, Svalbard, which, like many ice masses on Svalbard (cf. Sevestre and Benn, 2015; Farnsworth et al., 2016), is known to be surge-type (cf. Robinson and Dowdeswell, 2011, and references therein), and this would have implications for the ELA. Consequently, a numerical model-based precipitation-temperature (*P/T*) function specific to the LLS in Scotland has been proposed (eq. 2). The alternative *P/T* function permits an annual temperature range of 30°C, which is more consistent with evidence from palaeoclimatic proxies (e.g. Atkinson et al., 1987; Isarin et al., 1998; Witte et al., 1998; Lie and Paasche, 2006).

$$P = S(14.2T_a^2 + 248.2T_a + 213.5) \qquad (2)$$

where P is effective precipitation, T_a is the mean temperature (°C) of the ablation season, and S is the seasonality factor; S = 1 for neutral-type, S = 1.4 for summer-dominated or S = 0.8 winter-dominated precipitation (Golledge *et al*., 2010).

Both *P/T* functions are employed here to facilitate comparison with previous studies and between the two approaches. Quantitative estimates of palaeotemperatures during the LLS have been derived from chironomids at four sites in Scotland: (i) Whitrig Bog, SE Scotland (Brooks and Birks, 2000a); (ii) Abernethy Forest, Cairngorms (Brooks et al., 2012); (iii) Loch Ashik, Isle of Skye (Brooks et al., 2012); and (iv) Muir Park Reservoir (MPR) near Loch Lomond, west-central Scotland (Brooks et al., 2016). The closest site to BMC, Loch Ashik (~90 km to the SW), has yielded a July chironomid-inferred temperature (C-IT) of 6.9°C during the coldest part of the LLS stadial. However, the reliability of the estimates from this particular site is questionable as samples obtained from Loch Ashik had a poor fit-to-temperature, suggesting July air temperatures were not the main influence on chironomid distribution and abundance (Brooks et al., 2012). Moreover, the composition of the chironomid assemblages at Loch Ashik, and MPR, in the late LLS suggest these lakes were influenced by an influx of cold waters from snowbeds (cf. Brooks et al., 2012, 2016). This issue has also been observed in Norway (Brooks and Birks, 2000b; Velle et al., 2005), and chironomids are considered unreliable proxies for palaeotemperature in such cases (cf. Bjune et al., 2005). On this basis, we use a summer temperature at sea-level of 8.5 ± 0.3°C (mean July temperature) in accordance with recent studies elsewhere in Scotland (see Boston et al., 2015, and references therein, for further details). A second temperature value of 6.38°C is also employed, based on modelling experiments by Golledge et al. (2008). This value was suggested as an alternative that accounts for the effects of localised cooling of air temperatures by glaciers, unlike the C-IT value that is derived from ice-free areas.

In order to generate a mean summer (ablation season) temperature from the mean July temperature value of 8.5 ± 0.3°C, as necessitated by both *P/T* functions, a relationship proposed by Benn and Ballantyne (2005), based on analysis of meteorological data from Scotland and Scandinavia, was used:

$$T_a = 0.97T_j \qquad (3)$$

where T_a is the mean summer temperature and T_j is the mean July temperature (°C) at the ELA. It should be noted that this equation assumes that the current Scandinavian and Scottish summer climates are suitable analogues for LLS summer climate in Scotland. However, in the absence of any other data, the equation is considered a reasonable approximation and followed here. Using a mean July sea-level temperature of 8.5 ± 0.3°C and eqn. 3, and

assuming typical environmental lapse rates of 0.006–0.007°C m^{-1}, the mean summer temperature at the ELA of the BMC glaciers is 6.2 ± 0.4°C. An alternative temperature function has been advocated by Golledge et al. (2010) which incorporates the effect of local glacier cooling:

$$T_a = 0.97(T_j + 0.00205\Delta_e - 0.00373\Delta_n - 6.15\Delta_{alt}) - 10^{(0.28\log L - 0.07)} \quad (4)$$

where T_j is the July temperature for the coldest part of the LLS derived from an independent temperature proxy, Δ_e, Δ_n, and Δ_{alt} are, respectively, the easting, northing and altitudinal differences (km) with respect to the site used for T_j, and L is the length of the palaeoglacier (km). However, we have opted not to use this relationship as it would preclude direct comparison with previously published work for the region (Lukas and Bradwell, 2010), and it is not possible to consider the effect of glacier cooling on air temperature for the Sutherland icefield as a whole or complex outlets of the icefield (e.g. outlets with multiple source areas), since no single value can be obtained for glacier length (cf. Boston et al., 2015).

Applying the resulting palaeotemperature value to the *P/T* functions yielded palaeoprecipitation estimates of 2817 ± 425 mm a^{-1} using the Ohmura et al. (1992) equation (eq. 1), and 3204 ± 328 mm a^{-1}, 2288 ± 234 mm a^{-1} and 1831 ± 187 mm a^{-1} for the summer-, neutral- and winter-dominated precipitation types, respectively, using the Golledge et al. (2010) equation (eq. 2) (Table 2). The range of palaeoprecipitation values represent a variety of climatic regimes, highlighting the influence that seasonality could have upon glacier mass-balance (cf. Golledge et al., 2010; Finlayson et al., 2011).

To place these palaeoprecipitation values into context, a consideration of modern precipitation values is required. Mean annual precipitation for Ullapool [NC 126940; 12 m OD] was 1358 mm a^{-1} for the 22-year period between 1961 and 1984 for which the rainfall record was complete (British Atmospheric Data Centre). Since precipitation increases non-linearly with altitude (e.g. Ballantyne, 1983; Ward and Robinson, 1990), these values require adjustment to the LLS ELA to facilitate direct comparison. A modern precipitation value at the ELA can be derived from the following relationship (Ballantyne, 2002):

$$P_{Z1} = P_{Z2} / (1 + P^*)^{0.01(Z2 - Z1)} \quad (5)$$

475
476 where P_{Z1} and P_{Z2} represent the precipitation at altitudes Z1 and Z2, and P^* is the
477 proportional increase in precipitation per 100 m increase in elevation. Employing data from
478 Ben Nevis, Ballantyne (2002) has demonstrated that $P^* = 0.0578$, and this value is utilised
479 here. The relationship yields modern precipitation values of 1349 mm a^{-1} at sea level and
480 1621 ± 15 mm a^{-1} at the mean ELA (328 ± 16 m). By comparison, the sea-level equivalent
481 palaeoprecipitation estimates for BMC were 2343 ± 335 mm a^{-1} using the Ohmura et al.
482 (1992) equation, and 2665 ± 249 mm a^{-1}, 1903 ± 178 mm a^{-1} and 1523 ± 142 mm a^{-1} using
483 the Golledge et al. (2010) equation with summer-, neutral- and winter-type precipitation
484 seasonality, respectively (Table 2).
485
486 ***Potential snowblow and avalanche areas***
487
488 An assessment of the influence of topographically-enhanced snow accumulation appears
489 necessary as (i) windblown snow may have played a key role in glacier build-up during the
490 LLS in Scotland (cf. Golledge, 2010), (ii) plateau surfaces exist to the southwest of the
491 corries which could, conceivably, have contributed snow by both wind redistribution and
492 avalanching, and (iii) the association of gullies with flat expanses of the BMC massif and ice
493 accumulation zones implies that accumulation zones may have existed on the plateau (see
494 *'Palaeoglaciological reconstruction'*). Additionally, the corries are oriented leeward of the
495 dominant west-southwest airflow direction during the LLS, inferred from glacial and
496 periglacial evidence (e.g. Sissons, 1979a, b, 1980a; Ballantyne and Kirkbride, 1986;
497 Ballantyne, 1989, 2002) and from observations of *in situ* relict windpolished boulders and
498 bedrock (cf. Christiansen, 2004). Thus, the conditions appear propitious for topographically-
499 enhanced snow accumulation. If this was the case, any reconstructed ELAs would be lower
500 than the 'true' climatic ELA of adjacent ice masses (e.g. Nesje and Dahl, 2000; Benn and
501 Lehmkuhl, 2000; Coleman et al., 2009), thereby overestimating palaeo-precipitation. Hence,
502 we pay particular attention to a systematic assessment of this influence here.
503
504 Potential snowblow (PSBAs) and potential avalanche (PAAs) areas were established using
505 procedures outlined elsewhere (Mitchell, 1996), which are underpinned by the assumption
506 that all ground situated above the ELA, and laterally continuous to the palaeoglaciers, has the
507 potential to contribute snowblow or avalanching. Moreover, a maximum slope angle of 10°
508 for slopes dipping away from the glaciers is considered a threshold for snowblow,

acknowledging the possibility of steep slopes acting as snow fences (Robertson, 1989; Coleman et al., 2009). Slopes surrounding the reconstructed glaciers which exceed 20° are considered PAAs (Sissons and Sutherland, 1976). The snowblow areas established for the BMC corrie glaciers display a preferred orientation, with the largest potential snowblow areas to the south and southwest (Figure 8). The synthesised data (Table 3) indicate terrain in the southwest quadrant (181–270°) is the most important source of windblown snow, representing 76.3% (Cadh' a' Mhoraire), 88.6% (Sgùrr an Fhidleir) and 87.8% (An Clù-nead) of total snowblow area for the respective glaciers. The PSBAs evident in the southwest quadrant correlate with dominant palaeo-wind directions from the southwest; thus, implying that topographically enhanced snow accumulation augmented glacier mass balance.

The significance of these PSBAs can be assessed by calculation of the ratio of potential snowblow area to glacier area (Sissons, 1980a, b; Sutherland, 1984; Mitchell, 1996). However, not all PSBAs will have an equal opportunity to contribute snow, with areas situated further from the glacier being less likely to add snow to the glacier (cf. Mitchell, 1996; Mills et al., 2009, 2012). Sissons (1980a) suggested this issue could be circumvented by calculating 'snowblow factors' – the square root of the snowblow ratio – and this approach is followed here. Snowblow factors for the three BMC corrie glaciers (Table 3) are comparable to values presented for other sites in upland Britain (cf. Mitchell, 1996; Coleman et al., 2009).

The potential for avalanching onto the glacier surface appears most important for the Cadh' a' Mhoraire and An Clù-nead glaciers (Table 4). In all cases, the largest PAAs (SW quadrant) correspond with both the dominant snowblow areas and the prevailing wind direction during the LLS. The correlation evident between dominant PAAs, PSBAs and the prevailing palaeo-wind direction implies a plentiful supply of snow to the plateau which could, potentially, avalanche onto surface of the glaciers. Avalanche factors – calculated as the ratio of avalanche area to glacier area – for the BMC glaciers (Table 4) are similar to those presented for corrie glaciers elsewhere in the UK (cf. Coleman et al., 2009).

Discussion

Significance and implications of the gullies

Our geomorphological investigations at BMC have identified a number of striking deeply-incised gullies that are found in close association with moraines situated downvalley and plateau surfaces just upvalley. Based on these morphostratigraphic relationships, and the concentration of the deeply-incised gullies on the corrie headwalls, we argue that this is a glaciologically-significant association and propose that such features in glaciated landscapes provide an indicator of cold-based ice and/or snowfields on plateaux immediately upslope of these gullies. Glacier surface profile modelling also appears to provide support for plateau-based ice, though this could be explained by the limitations of the model in such settings (see *'Palaeoglaciological reconstruction'*). Nevertheless, we hypothesise that the gullies represent former proglacial or pronival channels, with the emergence of meltwater from the cold-based ice or snow patches leading to the incision of gullies on the BMC massif and similar features elsewhere (cf. Christiansen, 1996, 1998). The longer shaping of such features over several snowmelt seasons under cold-climate conditions that would have prevailed for some time after deglaciation at higher altitudes is likely to have contributed to the deep incisions. Furthermore, the development of snow cornices along the plateau edge may also have contributed to gully erosion both directly, through subnival fluvial erosion, and indirectly, by 'pre-conditioning' the plateau edge and enhancing fluvial erosion: observations on Svalbard demonstrate that snow cornices promote and trigger denudation (Eckerstorfer et al., 2013a, b). We have noted similar associations of cold-based ice connections and gullies elsewhere in a palaeoglaciological context (e.g. Brecon Beacons, Coire Ardair, Ffynnon Llugwy, the Gaick), suggesting that these may be prevalent features and that they could be used as an additional criterion for identifying cold-based plateau ice or semi-permanent ice in glaciated landscapes. Further research is, however, ongoing to explore this association in detail and future studies should give explicit consideration to deeply-incised gullies.

As a result of the uncertainty over the potential influence of plateau ice on mass balance, the average ELA of 328 ±16 m (AABR = 1.91 ± 0.81) calculated for the BMC palaeoglaciers should be regarded as a minimum. Indeed, the presence of cold-based plateau ice on the massif could have a considerable impact on the nature and dynamics of glaciation by substantially increasing the surface area of the accumulation zone and, consequently, increasing the ELA (cf. Boston et al., 2015, and references therein). Conversely, the presence of plateau ice would decrease palaeoprecipitation estimates derived from the ELA. This does, therefore, introduce uncertainty into the palaeoclimatic discussions.

Regional palaeoclimatic inferences

Comparison between palaeoprecipitation estimates derived from the BMC glaciers and those previously obtained for the nearby West Sutherland icefield (Lukas and Bradwell, 2010; recalculated by Boston et al., 2015) reveals comparable sea-level equivalent precipitation values (Table 5). Conversely, to the SE of BMC, palaeoprecipitation values yielded from the Beinn Dearg ice-cap (Finlayson et al., 2011; recalculated by Boston et al., 2015) imply much drier conditions compared with BMC (~26–53% reduction) and West Sutherland (~27–47% reduction) (Table 5). These glacier-derived precipitation estimates, therefore, suggest the existence of general S–N and W–E precipitation gradients in this part of Scotland during the LLS, irrespective of the precipitation function used or the seasonality applied. This is consistent with numerical modelling results which indicate strong zonal circulation with increased frequency of depressions, particularly in winter (Isarin et al., 1998; Renssen et al., 2001). Moreover, these precipitation gradients are necessary for numerical simulations of LLS ice masses to closely resemble empirical evidence (Golledge et al., 2008). Nevertheless, the BMC glaciers would be expected to yield lower palaeoprecipitation estimates than those obtained given the substantial S–N precipitation gradient between Beinn Dearg and West Sutherland, implying that topoclimatic factors may have augmented mass balance (discussed further below).

However, there are caveats that should be taken into consideration when interpreting these palaeoprecipitation estimates. Principally, the timing of glacier maxima is typically taken as coincident with the coldest part of the LLS; therefore, palaeotemperature values for that point in the stadial are utilised to derive palaeoprecipitation estimates (e.g. Benn and Ballantyne, 2005; Lukas and Bradwell, 2010; Boston et al., 2015). However, the build-up of glaciers integrates palaeoclimatic fluctuations over longer time periods and complex interactions between climate variables (cf. Lukas and Bradwell, 2010). Additionally, there is significant debate and much divergence regarding the timing of LLS maxima across Scotland (e.g. Golledge et al., 2008; Ballantyne, 2012; Palmer et al., 2010, 2012; MacLeod et al., 2011; Bromley et al., 2014, 2016; Small and Fabel, 2016a, b). By employing temperature estimates associated with the latter, colder part of the LLS, erroneously low palaeoprecipitation estimates may be obtained. Calculated palaeo-ELAs, which form the basis of palaeoprecipitation estimates, are also underpinned by the assumption that the reconstructed ice mass was in equilibrium with climate whilst at its maximum. It is, however, unlikely that

611 all glaciers within a region were in equilibrium at their maxima due to short-lived advances
612 (Roe, 2011). Moreover, outlets/sectors of an icefield and independent ice masses within the
613 same region are unlikely to have reached their maxima at the same time, owing to factors
614 such as catchment size and shape, glacier length, aspect and hypsometry (e.g. Lukas and
615 Benn, 2006; Barr and Lovell, 2014). These issues, therefore, add uncertainty to the glacier-
616 derived palaeoprecipitation estimates obtained in this and other studies.
617
618 ***Comparison of glacier-derived palaeoprecipitation with modern values***
619
620 For comparison with modern precipitation values, we have employed the neutral-seasonality
621 precipitation value, in view of uncertainties associated with seasonal precipitation bias and
622 the effect of glacier air temperature cooling (cf. Boston et al., 2015, for discussion), and
623 issues related to applying the Ohmura et al. (1992) global dataset (cf. Golledge et al., 2010;
624 Lukas and Bradwell, 2010, for discussion). To compare this LLS precipitation value to
625 present-day precipitation, both values need to be reduced to sea level (see *'Palaeoclimatic*
626 *reconstruction'*). Present-day precipitation totals at sea level are 1349 mm a^{-1}, ~22–35 %
627 lower than the corresponding LLS value (1903 ± 178 mm a^{-1}; AABR = 1.91 ± 0.81); thus,
628 implying wetter conditions during the LLS than the present day at BMC. However,
629 comparison of recalculated values for West Sutherland (1844 ± 362 mm a^{-1}; Boston et al.,
630 2015) with modern sea-level equivalent precipitation at Loch Merkland (1863 mm a^{-1}; Lukas
631 and Bradwell, 2010) indicates that LLS precipitation may have been between ~26% lower
632 and ~16% higher than the present day, when taking into account error values: the central
633 value is, however, indistinguishable from the present-day precipitation total. Moreover, the
634 glacier-derived precipitation estimates suggest that the modern S–N precipitation gradient
635 between Ullapool and Loch Merkland was not evident during the LLS, indicating that the
636 presence of the former ice masses may have ameliorated any scavenging effects of the
637 mountains evident today.
638
639 ***Influence of topoclimatic factors***
640
641 The wetter LLS climate implied by glacier-derived precipitation estimates for BMC
642 contradicts evidence that Scotland had a more arid climate during the LLS, with a short-lived,
643 relatively mild, summer ablation season (cf. Golledge et al., 2010; Palmer et al., 2012, and
644 references therein). This, combined with the absence of a precipitation gradient between

BMC and West Sutherland, suggests that the BMC corrie glaciers may not be purely reflective of regional palaeoclimate: the mass balance of the glaciers may have been augmented by topoclimatic factors, thereby lowering the ELA from the 'true' climatic ELA. An assessment of PSBAs has indicated that areas to the southwest of the corries could potentially have contributed snow. Moreover, the quadrant with the most potential for snowblow for each glacier (180–270°) corresponds with the dominant wind direction during the LLS (see *'Potential snowblow and avalanche areas'*). Thus, it appears that snowblow may have been a contributor to mass balance. Avalanching, while less important than snowblow, also appears to have augmented glacier mass balance at BMC, with the most important sectors corresponding to the dominant palaeo-wind direction. Modern process observations on Svalbard demonstrate cornice-fall avalanches are most frequently initiated in sectors associated with the prevailing wind direction: niveo-aeolian transport across the plateau allows the development of cornices along the plateau edge (Eckerstorfer and Christiansen, 2011). Therefore, the data presented here strongly suggest that the disparities in the precipitation estimates reflect the influence of topographically-enhanced snow accumulation. Moreover, the incidence of the eroded plateau rim and deeply-incised gullies at BMC appears to provide geomorphological evidence for the presence of snowpatches on the plateau, niveo-aeolian transport across the plateau and the development of snow cornices (cf. Christiansen, 1996, 1998; Eckerstorfer et al., 2013a, b), which in turn implies snowblow and avalanching contributions to glacier mass balance. Therefore, the data presented here suggest that the disparities in the precipitation estimates are highly likely to reflect the influence of topographically-enhanced snow accumulation. It is, however, difficult to quantify the influence of snowblow, and there are uncertainties associated with our analyses. Calculation of PSBAs was underpinned by the assumption that slopes with a maximum slope angle of greater than 10° act as snow fences (see *'Potential snowblow and avalanche areas'*), but contemporary observations on Svalbard indicate snowblow can operate efficiently across vertical slopes facing upwind (Humlum, 2002). Thus, the PSBAs established should be considered a conservative minimum, and further analyses of snowblow using more sophisticated modelling approaches (e.g. Harrison et al., 2014), combined with radiation modelling (e.g. Mills et al., 2012), would be beneficial.

The above discussion is, however, based upon palaeoprecipitation values derived from a corrie glacier configuration for BMC. As highlighted above, cold-based ice may have existed on the plateau to the southwest of the corries. A plateau-ice scenario could substantially raise

679 ELAs, thereby reducing palaeoprecipitation estimates. Thus, both the possibility of plateau-
680 ice and influence of snowblow warrant further research. Moreover, detailed
681 palaeoglaciological studies of other corries in NW Scotland may provide further insights into
682 the potential influence of topoclimatic factors.
683
684 **Conclusions**

685 The main findings of this research are as follows:

686 • Geomorphological mapping has revealed evidence, principally in the form of
687 prominent moraine assemblages, for glaciers that occupied three corries on the
688 northern side of the BMC massif.
689 • Coeval limits have been delineated for three locally-nourished cirque glaciers, which
690 have been ascribed to the LLS (≈Younger Dryas; ~12.9–11.7 ka) on the basis of
691 morphostratigraphic principles and lake sediment evidence from the wider region.
692 • Three-dimensional reconstructions of the three BMC glaciers were produced using a
693 combination of geomorphological evidence and a two-dimensional glacier surface
694 profile model.
695 • ELAs were reconstructed using the AAR and AABR methods, and were computed by
696 an ArcGIS ELA toolbox. Using an AABR of 1.91 ± 0.81 yields an average ELA of
697 328 ± 16 m for the three corrie glaciers, comparable to ELAs for nearby West
698 Sutherland icefield.
699 • However, our modelling of glacier surface profiles, and the incidence of deeply-
700 incised gullies eroded into corrie backwalls at BMC, suggests that non-erosive, cold-
701 based ice may have existed on the plateau to the south of the corries. As such, we
702 consider the reconstructed ELAs as a minimum at this stage. Nonetheless, uncertainty
703 over the extent of any plateau-based ice precludes the reconstruction of its three-
704 dimensional form.
705 • Assuming a July summer sea-level temperature of 8.5 ± 0.3°C, LLS precipitation is
706 estimated to have been 2343 ± 335 mm a^{-1} using the Ohmura et al. (1992) equation
707 and 2665 ± 249 mm a^{-1}, 1903 ± 178 mm a^{-1} and 1523 ± 142 mm a^{-1} using the
708 Golledge et al. (2010) equation with summer-, neutral- and winter-type precipitation
709 seasonality, respectively. There are still debates regarding seasonality bias and the
710 most applicable precipitation function, but we employed the neutral-type precipitation

value for comparison with modern precipitation totals. Using this value, we demonstrate that precipitation was ~22–35% greater than the present-day values of 1349 mm a^{-1} at sea level. This data contrasts with assertions in recent studies that the LLS experienced drier conditions than the present-day.

- Comparison with recalculated values from the West Sutherland icefield reveal similar precipitation totals and indicates BMC does not conform to the expected S–N regional precipitation gradient. We argue on the basis of snowblow and avalanching analyses that these discrepancies reflect topographically-enhanced snow accumulation: snowblow and avalanching augmented mass balance, thereby lowering the ELA from the 'true' climatic ELA. Nevertheless, further analyses of snowblow, both at BMC and sites elsewhere in NW Scotland, using more sophisticated modelling approaches would be beneficial and provide greater insights into the influence of topoclimatic factors.
- Our findings highlight the importance of assessing the influence of topoclimatic factors when applying small (corrie) glaciers in palaeoclimatic reconstructions and show that such systematic assessments can elucidate complexities in regional palaeoclimate trends, namely precipitation gradients.

Acknowledgements

We are grateful to the British Geological Survey and Steve Brooks who kindly provided access to aerial photographs and chironomid-inferred temperature data, respectively. Thanks are also due to the UK Meteorological Office and British Atmospheric Data Centre for access to modern precipitation data. The NEXTMap Britain dataset for the study area was licensed to BMPC by NEODC under a Demonstration User License Agreement. BMPC would like to thank Jonathan Chandler, for his company and assistance in the field, and Simon Carr, for stimulating discussions at the outset of this project. SL is grateful to Hanne Christiansen and Ole Humlum for detailed discussions about nivation and gullying. We thank Iestyn Barr and an anonymous reviewer for their comments on an earlier version of this manuscript.

Abbreviations

AAR, accumulation area ratio; AABR, area-altitude balance ratio; AWMA, area-weighted mean altitude; BMC, Ben More Coigach, BR, balance ratio; C-IT, chironomid-inferred temperature; ELA, equilibrium line altitude; GSD, Ground Sampled Distance; LLS, Loch Lomond Stadial; MPR, Muir Park Reservoir; PAAs, potential avalanche areas; PSBAs, potential snowblow areas

References

Atkinson TC, Briffa KR, Coope, GR. 1987. Seasonal temperatures in Britain during the past 22 000 years, reconstructed using beetle remains. *Nature* **325**: 587–592.

Bakke J, Dahl SO, Nesje A. 2005a. Lateglacial and early Holocene palaeoclimatic reconstruction based on glacier fluctuations and equilibrium-line altitudes at northern Folgefonna, Hardanger, western Norway. *Journal of Quaternary Science* **20**: 179–198.

Bakke J, Dahl SO, Paasche Ø, Reidar L, Nesje A. 2005b. Glacier fluctuations, equilibrium-line altitudes and palaeoclimate in Lyngen, northern Norway, during the Lateglacial and Holocene. *The Holocene* **15**: 518–540.

Ballantyne CK. 1983. Precipitation gradients in Wester Ross, north-west Scotland. *Weather* **38**: 379–387.

Ballantyne CK. 1988. Ice-sheet moraines in southern Skye. Scottish Journal of Geology **24**: 301–304.

Ballantyne CK. 1989. The Loch Lomond Readvance on the Isle of Skye, Scotland: glacier reconstruction and palaeoclimatic implications. *Journal of Quaternary Science* **4**: 95–108.

Ballantyne CK. 1991. Holocene geomorphic activity in the Scottish Highlands. *Scottish Geographical Magazine* **107**: 84–98.

Ballantyne CK. 1995. Periglacial features of Assynt and Coigach. In *The Quaternary of Assynt and Coigach: Field Guide*, Lawson TJ (ed). Quaternary Research Association: London; 47–60.

Ballantyne CK. 2002. The Loch Lomond Readvance on the Isle of Mull, Scotland: glacier reconstruction and palaeoclimatic implications. *Journal of Quaternary Science* **17**: 759–771.

Ballantyne CK. 2007a. The Loch Lomond Readvance on north Arran, Scotland: glacier reconstruction and palaeoclimatic implications. *Journal of Quaternary Science* **22**: 343–359.

Ballantyne CK. 2007b. Loch Lomond Stadial glacier on North Harris, Outer Hebrides, North-West Scotland: glacier reconstruction and palaeoclimatic implications. *Quaternary Science Reviews* **26**: 3134–3149.

Ballantyne CK. 2012. Chronology of glaciation and deglaciation during the Loch Lomond (Younger Dryas) Stade in the Scottish Highlands: implications of recalibrated 10Be exposure ages. *Boreas* **41**(4): 513–526.

778 Ballantyne CK, Eckford JD. 2008. Characteristics and evolution of two relict talus slopes in Scotland.
779 *Scottish Geographical Magazine* **100**: 20–33.
780 Ballantyne CK, Hall AM, Phillips W, Binnie S, Kubik PW. 2007. Age and significance of former
781 low-altitude corrie glaciers on Hoy, Orkney Islands. *Scottish Journal of Geology* **43**: 107–
782 114.
783 Ballantyne CK, Harris C. 1994. *The Periglaciation of Great Britain*. Cambridge University Press:
784 Cambridge; 330 p.
785 Ballantyne CK, Kirkbride MP. 1986. The characteristics and significance of some lateglacial protalus
786 ramparts in upland Britain. *Earth Surface Processes and Landforms* **11**: 659–671.
787 Barr ID, Lovell H. 2014. A review of topographic controls on moraine distribution. *Geomorphology*
788 **226**: 44–64.
789 Bendle JM, Glasser NF. 2012. Palaeoclimatic reconstruction from Lateglacial (Younger Dryas
790 Chronozone) cirque glaciers in Snowdonia, North Wales. *Proceedings of the Geologists'*
791 *Association* **123**: 130–145.
792 Benn DI. 1997. Glacier fluctuations in western Scotland. *Quaternary International* **38/39**: 137–47.
793 Benn DI, Ballantyne CK. 2005. Palaeoclimatic reconstruction from Loch Lomond Readvance glaciers
794 in the West Drumochter Hills, Scotland. *Journal of Quaternary Science* **20**: 577–592.
795 Benn DI, Gemmell, AMD. 1997. Calculating equilibrium-line altitudes of former glaciers by the
796 balance ratio method: a new computer spreadsheet. *Glacial Geology and Geomorphology*.
797 Available from: http://ggg.qub.ac.uk/papers/full/1997/tn011997/tn01.html
798 Benn DI, Hulton, NRJ. 2010. An Excel™ spreadsheet program for reconstructing the surface profile
799 of former mountain glaciers and ice caps. *Computers & Geosciences* **36**: 605–610.
800 Benn DI, Lehmkuhl F. 2000. Mass balance and equilibrium-line altitudes of glaciers in high-mountain
801 environments. *Quaternary International* **65–66**, 15–29.
802 Benn DI, Lowe JJ, Walker MJC. 1992. Glacier response to climatic change during the Loch Lomond
803 Stadial and early Flandrian: geomorphological and palynological evidence from the Isle of
804 Skye, Scotland. *Journal of Quaternary Science* **7**, 125–144.
805 Benn DI, Lukas S. 2006. Younger Dryas glacial landsystems in North West Scotland: an assessment
806 of modern analogues and palaeoclimatic implications. *Quaternary Science Reviews* **25**: 2390–
807 2408.
808 Benn DI, Owen LA, Osmaston HA, Seltzer GO, Porter SC, Mark B. 2005. Reconstruction of
809 equilibrium-line altitudes for tropical and sub-tropical glaciers. *Quaternary International*
810 **138–139**: 8–21.
811 Bennett MR. 1999. Paraglacial and periglacial slope adjustment of a degraded lateral moraine in Glen
812 Torridon. *Scottish Journal of Geology* **35**: 79–83.

Bickerdike HL, Evans DJA, Ó Cofaigh C, Stokes CR. 2016. The glacial geomorphology of the Loch Lomond Stadial in Britain: a map and geographic information system resource of published evidence. *Journal of Maps* **12**(5): 1178–1186.

Björck S, Bennike O, Rosén P, Andresen CS, Bohncke S, Kaas E, Conley D. 2002. Anomalously mild Younger Dryas summer conditions in southern Greenland. *Geology* **30**: 427–430.

Bjune AE, Bakke J, Nesje A, Birks HJB. 2005. Holocene mean July temperature and winter precipitation in western Norway inferred from palynological and glaciological lake-sediment proxies. *The Holocene* **15**: 177–89.

Boston CM. 2012. A glacial geomorphological map of the Monadhliath Mountains, Central Scottish Highlands. *Journal of Maps* **8**(4): 437–444.

Boston CM, Lukas S. 2016. Evidence for restricted Loch Lomond Stadial plateau ice in Glen Turret and implications for the age of the Turret Fan. *Proceedings of the Geologists' Association*, in press. doi: 10.1016/j.pgeola.2016.03.008

Boston CM, Lukas S, Carr SJ. 2015. A Younger Dryas plateau icefield in the Monadhliath, Scotland, and implications for regional palaeoclimate. *Quaternary Science Reviews* **108**: 139–162.

Bradwell T. 2006. The Loch Lomond Stadial glaciation in Assynt: A reappraisal. *Scottish Geographical Journal* **122**: 274–292.

Bradwell T, Stoker M, Krabbendam M. 2008. Megagrooves and streamlined bedrock in NW Scotland: The role of ice streams in landscape evolution. *Geomorphology* **97**: 135–156.

Bradwell T, Stoker MS, Golledge NR, Wilson CK, Merritt JW, Long D, Everest JD, Hestvik OB, Stevenson AG, Hubbard AL, Finlayson AG, Mathers HE. 2008. The northern sector of the last British Ice Sheet: Maximum extent and demise. *Earth-Science Reviews* **88**: 207–226.

Bradwell T, Stoker M, Larter R. 2007. Geomorphological signature and flow dynamics of The Minch palaeo-ice stream, northwest Scotland. *Journal of Quaternary Science* **22**: 609–617.

Bromley GR, Putnam AE, Rademaker KM, Lowell TV, Schaefer JM, Hall B, Winckler G, Birkel SD, Borns HW. 2014. Younger Dryas deglaciation of Scotland driven by warming summers. *Proceedings of the National Academy of Sciences of the United States of America* **111**: 6215–6219.

Bromley GRM, Putnam AE, Lowell TV, Hall BL, Schaefer, JM. 2016. Comment on 'Was Scotland deglaciated during the Younger Dryas?' by Small and Fabel (2016). *Quaternary Science Reviews* **152**: 203–206.

Brooks SJ, Birks HJB. 2000a. Chironomid-inferred Late-glacial air temperatures at Whitrig Bog, Southeast Scotland. *Journal of Quaternary Science* **15**: 759–764.

Brooks SJ, Birks HJB. 2000b. Chironomid-inferred lateglacial and early-Holocene mean July air temperatures for Kråkenes Lake, western Norway. *Journal of Paleolimnology* **23**: 77–89.

Brooks SJ, Davies KL, Mather KA, Matthews IP, Lowe JJ. 2016. Chironomid-inferred summer temperatures for the Last Glacial-Interglacial Transition from a lake sediment sequence in Muir Park Reservoir, west-central Scotland. *Journal of Quaternary Science* **31**: 214–224.

Brooks SJ, Matthews IP, Birks HH, Birks HJB. 2012. High resolution Lateglacial and early-Holocene summer air temperature records from Scotland inferred from chironomid assemblages. *Quaternary Science Reviews* **41**: 67–82.

Brown IM. 1993. Pattern of deglaciation of the last (Late Devensian) Scottish ice sheet: evidence from ice-marginal deposits in the Dee valley, northeast Scotland. *Journal of Quaternary Science* **8**: 235–50.

Carr S. 2001. A glaciological approach for the discrimination of Loch Lomond Stadial glacial landforms in the Brecon Beacons, South Wales. *Proceedings of the Geologists' Association* **112**: 253–261.

Carr SJ, Lukas S, Mills SC. 2010. Glacier reconstruction and mass-balance modelling as a geomorphic and palaeoclimatic tool. *Earth Surface Processes and Landforms* **35**: 1103–1115.

Chambers R. 1853. On the glacial phenomena in Scotland and Parts of England. *The Edinburgh New Philosophical Journal* **54**: 229–281.

Chandler BMP. 2013. *Glacial geomorphology of Ben More Coigach, Northwest Scottish Highlands: Implications for Loch Lomond Stadial glaciation and palaeoclimate*. Unpublished BSc Dissertation, Queen Mary University of London, 126 pp.

Chandler BMP, Evans DJA, Roberts DH, Ewertowski M, Clayton AI. 2015. Glacial geomorphology of the Skálafellsjökull foreland, Iceland: A case study of 'annual' moraines. *Journal of Maps* **12**(5): 904–916.

Charlesworth JK. 1955. Late-glacial history of the Highlands and Islands of Scotland. *Transactions of the Royal Society of Edinburgh* **62**: 769–928.

Christiansen HH. 1996. Effects of Nivation on Periglacial Landscape Evolution in Western Jutland, Denmark. *Permafrost and Periglacial Processes* **7**: 111–138.

Christiansen HH. 1998. Nivation forms and processes in unconsolidated sediments, NE Greenland. *Earth Surface Processes and Landforms* **23**: 751–760.

Christiansen HH. 2004. Windpolished boulders and bedrock in the Scottish Highlands: evidence and implications of Late Devensian wind activity. *Boreas* **33**: 82–94.

Coleman CG, Carr SJ, Parker AG. 2009. Modelling topoclimatic controls on palaeoglaciers: implications for inferring palaeoclimate from geomorphic evidence. *Quaternary Science Reviews* **28**: 249–259.

Darvill CM, Stokes CR, Bentley MR, Lovell H. 2014. A glacial geomorphological map of the southernmost ice lobes of Patagonia: the Bahía Inútil – San Sebastián, Magellan, Otway, Skyring and Río Gallegos lobes. *Journal of Maps* **10**(3): 500–520.

884 Eckerstorfer M, Christiansen HH. 2011. Topographical and meteorological control on snow
885 avalanching in the Longyearbyen area, central Svalbard 2006–2009. *Geomorphology* **134**:
886 186–196.
887 Eckerstorfer M, Christiansen HH, Rubensdotter L, Vogel S. 2013. The geomorphological effect of
888 cornice fall avalanches in the Longyeardalen valley, Svalbard. *The Cryosphere* **7**: 1361–1374.
889 Eckerstorfer M, Christiansen HH, Vogel S, Rubensdotter L. 2013. Snow cornice dynamics as a
890 control on plateau edge erosion in central Svalbard. *Earth Surface Processes and Landforms*
891 **38**: 466–476.
892 Ewertowski MW, Evans DJA, Roberts DH, Tomczyk AM. 2016. Glacial geomorphology of the
893 terrestrial margins of the tidewater glacier, Nordenskiöldbreen, Svalbard. *Journal of Maps*, in
894 press. doi: 10.1080/17445647.2016.1192329
895 Farnsworth WR, Ingólfsson Ó, Retelle M, Schomacker A. 2016. Over 400 previously undocumented
896 Svalbard surge-type glaciers identified. *Geomorphology* **264**: 52–60.
897 Finlayson AG. 2006. Glacial geomorphology of the Creag Meagaidh Massif, Western Grampian
898 Highlands: Implications for local glaciation and palaeoclimate during the Loch Lomond
899 Stadial. *Scottish Geographical Journal* **122**: 293–307.
900 Finlayson AG, Golledge N, Bradwell T, Fabel D. 2011. Evolution of a Lateglacial mountain icecap in
901 northern Scotland. *Boreas* **40**: 536–554.
902 Furbish DJ, Andrews JT. 1984. The use of hypsometry to indicate long-term stability and response of
903 valley glaciers to changes in mass transfer. *Journal of Glaciology* **30**: 199–211.
904 Golledge NR. 2008. *Glacial geology and glaciology of the Younger Dryas ice cap in Scotland*.
905 Unpublished PhD thesis, University of Edinburgh.
906 Golledge NR. 2010. Glaciation of Scotland during the Younger Dryas stadial: a review. *Journal of*
907 *Quaternary Science* **25**: 550–566.
908 Golledge NR, Hubbard A, Bradwell T. 2010. Influence of seasonality on glacier mass balance, and
909 implications for palaeoclimate reconstructions. *Climate Dynamics* **35**: 757–770.
910 Golledge NR, Hubbard A, Sugden DE. 2008. High-resolution numerical simulation of Younger Dryas
911 glaciation in Scotland. *Quaternary Science Reviews* **27**: 888–904.
912 Goodenough KM, Krabbendam M, Bradwell T, Finlayson A, Leslie AG. 2009. Digital surface models
913 and the landscape: interaction between bedrock and glacial geology in the Ullapool area.
914 *Scottish Journal of Geology* **45**: 99–105.
915 Gray JM. 1982. The last glaciers (Loch Lomond Advance) in Snowdonia, N. Wales. *Geological*
916 *Journal* **17**: 113–133.
917 Harrison S, Rowan AV, Glasser NF, Knight J, Plummer MA, Mills SC. 2014. Little Ice Age glaciers
918 in Britain: Glacier–climate modelling in the Cairngorm mountains. *The Holocene* **24**(2): 135–
919 140.

Hinchliffe S, Ballantyne CK. 2009. Talus structure and evolution on sandstone mountains in NW Scotland. *The Holocene* **19**: 477–486.

Hubbard B, Glasser NF. 2005. *Field techniques in glaciology and glacial geomorphology*. John Wiley and Sons: Chichester; 400 p.

Hughes PD. 2002. Loch Lomond Stadial glaciers in the Aran and Arenig Mountains, North Wales, Great Britain. *Geological Journal* **37**: 9–15.

Humlum O. 2002. Modelling late 20th-century precipitation in Nordenskiöld Land, Svalbard, by geomorphic means. *Norsk Geografisk Tidsskrift – Norwegian Journal of Geography* **56**: 96–103.

Intermap Technologies, 2007. NEXTMap Britain: Digital Terrain Mapping of the UK. NERC Earth Observation Data Centre. Available from: http://badc.nerc.ac.uk/view/neodc.nerc.ac.uk__ATOM__dataent_11658383444211836

Isarin RFB, Renssen H, Vandenberghe J. 1998. The impact of the North Atlantic Ocean on the Younger Dryas climate in northwestern and central Europe. *Journal of Quaternary Science* **13**: 447–453.

Johnstone GS, Mykura W. 1989. *British Regional Geology: The Northern Highlands* (4th Edition). British Geological Survey, HMSO: Edinburgh.

Jones RS, Lowe JJ, Palmer AP, Eaves SR, Golledge NR. 2015. Dynamics and palaeoclimatic significance of a Loch Lomond Stadial glacier: Coire Ardair, Creag Meagaidh, Western Highlands, Scotland. *Proceedings of the Geologists' Association*, in press. doi: 10.1016/j.pgeola.2015.11.004

Jost A, Lunt D, Kageyama M, Abe-Ouchi A, Peyron O, Valdes PJ, Ramstein G. 2005. High-resolutions simulations of the last glacial maximum climate over Europe: a solution to discrepancies with continental palaeoclimate reconstructions? *Climate Dynamics* **24**: 577–590.

Kirkbride MP, Mitchell WA, Barnes M. 2015. Reconstruction and Regional Significance of the Coire Breac Palaeoglacier, Glen Esk, Eastern Grampian Highlands, Scotland. *Geografiska Annaler* **97A**: 563–577.

Lawson TJ. 1986. Loch Lomond Advance glaciers in Assynt, Sutherland, and their palaeoclimatic implications. *Scottish Journal of Geology* **26**: 25–32.

Lawson TJ. (ed) 1995. *The Quaternary of Assynt and Coigach: Field Guide*. Quaternary Research Association: London; 162 p.

Lie O, Paasche O. 2006. How extreme was northern hemisphere seasonality during the Younger Dryas? *Quaternary Science Reviews* **25**: 404–407.

Lukas S. 2005a. A test of the englacial thrusting hypothesis of 'hummocky' moraine formation: case studies from the northwest Highlands, Scotland. *Boreas* **34**: 287–307.

Lukas S. 2005b. *Younger Dryas moraines in the NW Highlands of Scotland: genesis, significance and potential modern analogues*. Unpublished PhD thesis, University of St Andrews.

Lukas S. 2006. Morphostratigraphic principles in glacier reconstruction: a perspective from the British Younger Dryas. *Progress in Physical Geography* **30**: 719–736.

Lukas S, Benn DI. 2006. Retreat dynamics of Younger Dryas glacier in the far NW Scottish Highlands reconstructed from moraine sequences. *Scottish Geographical Journal* **122**: 308–325.

Lukas S, Bradwell T. 2010. Reconstruction of a Lateglacial (Younger Dryas) mountain ice field in Sutherland, northwestern Scotland, and its palaeoclimatic implications. *Journal of Quaternary Science* **25**: 567–580.

Lukas S, Lukas T. 2006. A glacial geological and geomorphological map of the far NW Highlands, Scotland. Parts 1 and 2. *Journal of Maps* **2006**: 43–56, 56–58.

MacLeod A, Palmer A, Lowe J, Rose J, Bryant C, Merritt J. 2011. Timing of glacier response to Younger Dryas climatic cooling in Scotland. *Global and Planetary Change* **79**: 264–274.

Meierding TC. 1982. Late Pleistocene glacial equilibrium-line altitudes in the Colorado Front Range – a comparison of methods. *Quaternary Research* **18**: 289–310.

Mills SC, Grab SW, Carr SJ. 2009. Recognition and palaeoclimatic implications of late Quaternary niche glaciation in eastern Lesotho. *Journal of Quaternary Science* **24**: 647–663.

Mills SC, Grab SW, Rea BR, Carr SJ, Farrow A, 2012. Shifting westerlies and precipitation patterns during the Late Pleistocene in southern Africa determined using glacier reconstruction and mass balance modelling. *Quaternary Science Reviews* **55**: 145–159.

Mitchell WA. 1996. Significance of snowblow in the generation of Loch Lomond Stadial (Younger-Dryas) glaciers in the western Pennines, northern England. *Journal of Quaternary Science* **11**: 233–248.

Nesje A, Dahl SO. 2000. *Glaciers and Environmental Change*. Arnold: London; 203 p.

Ohmura A, Kasser P, Funk M. 1992. Climate at the equilibrium line of glaciers. *Journal of Glaciology* **38**: 397–411.

Osmaston H. 2005. Estimates of glacier equilibrium line altitudes by the Area×Altitude, the Area×Altitude Balance Ratio and the Area×Altitude Balance Index methods and their validation. *Quaternary International* **138–139**: 22–31.

Palmer AP, Rose J, Lowe JJ, MacLeod A. 2010. Annually resolved events of younger Dryas glaciation in Lochaber (Glen Roy and Glen Spean), western Scottish Highlands. *Journal of Quaternary Science* **25**: 581–596.

Palmer AP, Rose J, Rasmussen SO. 2012. Evidence for phase-locked changes in climate between Scotland and Greenland during GS-1 (Younger Dryas) using micromorphology of glaciolacustrine varves from Glen Roy. *Quaternary Science Reviews* **36**: 114–123.

992 Peach BN, Horne J. 1892. The ice-shed in the North-West Highlands during the maximum glaciation.
993 *Report of the British Association for 1892* 720.
994 Peach BN, Horne, J., Gunn, W., Clough, C.T., Hinxman, L.W., Teall, J.J.H., 1907. *The geological*
995 *structure of the North-West Highlands of Scotland. Memoir of the Geological Survey of Great*
996 *Britain*. HMSO: Edinburgh.
997 Pearce D. 2014. *Reconstruction of Younger Dryas glaciation in the Tweedsmuir Hills, Southern*
998 *Uplands, Scotland: Style, dynamics and palaeo-climatic implications*. Unpublished PhD
999 thesis, University of Worcester, 231 p.
1000 Pearce D, Rea BR, Bradwell T, McDougall D. 2014. Glacial geomorphology of the Tweedsmuir
1001 Hills, Central Southern Uplands, Scotland. *Journal of Maps* **10**(3): 457–465.
1002 Pellitero R, Rea BR, Spagnolo M, Bakke J, Hughes P, Ivy-Ochs S, Lukas S, Ribolini A. 2015. A GIS
1003 tool for automatic calculation of glacier equilibrium-line altitudes. *Computers & Geosciences*
1004 **82**: 55–62.
1005 Pellitero R, Rea BR, Spagnolo M, Bakke J, Ivy-Ochs S, Frew CR, Hughes P, Ribolini A, Lukas S,
1006 Renssen H. 2016. GlaRe, a GIS tool to reconstruct the 3D surface of palaeoglaciers.
1007 *Computers & Geosciences* **94**: 77–85.
1008 Pennington W. 1977. Lake sediments and the Lateglacial environment in northern Scotland. In
1009 *Studies in the Scottish Lateglacial environment*, Gray JM, Lowe JJ. (eds). Permagon Press:
1010 Oxford; 119–141.
1011 Pennington W, Haworth EY, Bonny AP, Lishman JP. 1972. Lake sediments in northern Scotland.
1012 *Philosophical Transactions of the Royal Society of London* **B264**: 191–294.
1013 Porter SC. 1975. Equilibrium-line altitudes of late Quaternary glaciers in the Southern Alps, New
1014 Zealand. *Quaternary Research* **5**: 27–47.
1015 Rea BR. 2009. Defining modern day Area-Altitude Balance Ratios (AABRs) and their use in glacier-
1016 climate reconstructions. *Quaternary Science Reviews* **28**: 237–248.
1017 Renssen H, Podzun R, Vandenberghe J, Isarin RFB, Jacob D. 2001. Simulation of the Younger Dryas
1018 climate in Europe using a regional climate model nested in an AGCM: preliminary results.
1019 *Global and Planetary Change* **30**: 41–57.
1020 Robertson DW. 1989. *Aspects of the Lateglacial and Flandrian environmental history of the Brecon*
1021 *Beacons, Fforest Fawr, Black Mountain and Abergavenny Black Mountains, South Wales*
1022 *(with emphasis on the Lateglacial and Early Flandrian periods*. Unpublished PhD thesis,
1023 University of Wales.
1024 Robinson M, Ballantyne CK. 1979. Evidence for a glacial readvance pre-dating the Loch Lomond
1025 Advance in Wester Ross. *Scottish Journal of Geology* **15**: 271–277.
1026 Robinson P, Dowdeswell JA. 2011. Submarine landforms and the behavior of a surging ice cap since
1027 the last glacial maximum: The open-marine setting of eastern Austfonna, Svalbard. *Marine*
1028 *Geology* **286**(1): 82–94.

1029 Roe GH. 2011. What do glaciers tell us about climate variability and climate change? *Journal of*
1030 *Glaciology* **57**: 567-578.
1031 Sevestre H, Benn DI. 2015. Climatic and geometric controls on the global distribution of surge-type
1032 glaciers: implications for a unifying model of surging. *Journal of Glaciology* **61**: 646–662.
1033 Sissons JB. 1974. A Late-glacial ice cap in the central Grampians, Scotland. *Transactions of the*
1034 *Institute of British Geographers* **62**: 95–114.
1035 Sissons JB. 1976. *The geomorphology of the British Isles: Scotland*. London: Methuen; 147 p.
1036 Sissons JB. 1977. The Loch Lomond Readvance in the northern mainland of Scotland. In *Studies in*
1037 *the Scottish Lateglacial Environment*, Gray JM. Lowe JJ. (eds). Permagon Press: Oxford; 45–
1038 60.
1039 Sissons JB. 1979a. The Loch Lomond Stadial in the British Isles. *Nature* **280**: 199–203.
1040 Sissons JB. 1979b. Palaeoclimatic inferences from former glaciers in Scotland and the Lake District.
1041 *Nature* **278**: 518–521.
1042 Sissons JB. 1980a. Palaeoclimatic inferences from Loch Lomond advance glaciers. In *Studies in the*
1043 *Lateglacial of North West Europe*, Lowe JJ, Gray JM, Robinson DE. (eds). Pergamon Press:
1044 Oxford; 31–43.
1045 Sissons, JB. 1980b. The Loch Lomond Advance in the Lake District, northern England. *Transactions*
1046 *of the Royal Society of Edinburgh, Earth Sciences* **71**: 13–27.
1047 Sissons JB, Sutherland DG. 1976. Climatic inferences from former glaciers in the south-east
1048 Grampian Highlands, Scotland. *Journal of Glaciology* **17**: 325-346.
1049 Small D, Fabel D. 2016a. Was Scotland deglaciated during the Younger Dryas? *Quaternary Science*
1050 *Reviews* **145**: 259–263.
1051 Small, D., Fabel, D., 2016b. Response to Bromley et al. "Comment on 'Was Scotland deglaciated
1052 during the Younger Dryas?' By Small and Fabel (2016)". *Quaternary Science Reviews* **152**:
1053 206–208.
1054 Stoker M, Bradwell T. 2005. The Minch palaeo-ice stream, NW sector of the British–Irish ice sheet.
1055 *Journal of the Geological Society of London* **163**: 423–428.
1056 Stuiver M, Reimer PJ, Reimer RW. 2016. CALIB radiocarbon calibration, version 7.1. Available at:
1057 http://calib.qub.ac.uk/calib/
1058 Sutherland DG. 1984. Modern glacier characteristics as a basis for inferring former climates with
1059 particular reference to the Loch Lomond Stadial. *Quaternary Science Reviews* **3**: 291–309.
1060 Thorp PW. 1986. A mountain icefield of Loch Lomond Stadial age, western Grampians, Scotland.
1061 *Boreas* **15**: 83–97.
1062 Torsnes I, Rye N, Nesje A. 1993. Modern and Little Ice Age Equilibrium-Line Altitudes on Outlet
1063 Valley Glaciers fromJostedalsbreen, Western Norway: An Evaluation of Different
1064 Approaches to Their Calculation. *Arctic and Alpine Research* **25**: 106–116.

Velle G, Larsen J, Eide W, Peglar SM, Birks HJB. 2005. Holocene environmental history and climate at Råtåsjøen, a low alpine lake in central Norway. *Journal of Paleolimnology* **33**(2): 129–153.

Ward RC, Robinson M. 1990. *Principles of Hydrology* (3rd Edition). McGraw-Hill: London; 365 p.

Witte HJL, Coope GR, Lemdahl G, Lowe JJ. 1998. Regression coefficients of thermal gradients in northwestern Europe during the last glacial–Holocene transition using beetle MCR data. *Journal of Quaternary Science* **13**: 435–445.

Figure captions

Figure 1. Digital Terrain Model (DTM) of Northwest Scotland, showing the regional context of the study site and its proximity to the West Sutherland mountain icefield (Lukas and Bradwell, 2010). Hill shaded relief map derived from DTM of NEXTMap Britain (Intermap Technologies Inc. provided by NERC via the Earth Observation Data Centre).

Figure 2. Location and relief of the Ben More Coigach massif, NW Scottish Highlands. Proposed Loch Lomond Stadial glaciers are digitised from Sissons (1977), with surface contours added at 10 m intervals. Orientation and scale are given by British National Grid coordinates (grid square NC). Elevation data derived from the NEXTMap Britain dataset (Intermap Technologies Inc. provided by NERC via the Earth Observation Data Centre).

Figure 3. Glacial geomorphological map of the study area, with particular reference to glacial landforms associated with the three corries on the northern side of the Ben More Coigach massif. Grid coordinates correspond to British National Grid tile NC. Contour lines and water bodies (c) Crown Copyright. Ordnance Survey an EDINA Digimap/JISC supplied service.

Figure 4. Oblique field photograph of the Cadh' a' Mhoraire moraines, viewed from the high ground to the east of the Sgùrr an Fhidleir summit [NC 094054].

Figure 5. Field photos showing the contrast between landform associations inside (A–B) and outside (C–D) the inferred glacial limits. (A) Ground view of the nested moraines in front of Cadh' a' Mhoraire and associated glacially-transported boulders, which align to form a boulder dispersal train on the eastern side of the corrie (B). These features contrast with the geomorphology beyond the limits of the moraine assemblages, which are characterised by bedrock outcrops (C), which may be ice-moulded in places, and debris-mantled slopes (D).

Figure 6. Modelled glacier surface profiles for the Ben More Coigach glaciers, based on Benn and Hulton (2010). (A)–(C) Modelled surface profiles where the glaciers are forced to intercept the corrie backwalls (i.e. shear stress = 0 kPa on the plateau). Despite imposed boundary conditions, the model predicts that ice could have existed on the plateau surface above the (B) Sgùrr an Fhidleir corrie. (D)–(F) Modelled glacier surface profiles where no boundary conditions were imposed, other than the surface gradient imposed by the moraines.

The modelling suggests that non-erosive, cold-based ice could have existed on the plateau to the southwest of the corries.

Figure 7. Three-dimensional reconstructions of the Ben More Coigach glaciers. Glacier 1 = Cadh' a' Mhoraire; Glacier 2 = Sgùrr an Fhidleir; 3 = An Clù-nead. Contour lines and water bodies © Crown Copyright. Ordnance Survey an EDINA Digimap/JISC supplied service.

Figure 8. Distribution of potential snowblow and avalanche areas around the Ben More Coigach glaciers, produced using the approach of Mitchell (1996). *N/I* indicates areas not included in the calculations.

Tables

Table 1. Equilibrium line altitudes (ELAs) calculated for the Ben More Coigach glaciers using the ArcGIS toolbox (Pellitero et al., 2015). Bold values indicate ELAs used for subsequent palaeoglaciological and palaeoclimatic calculations.

	Size (km^2)	ELA1 AABR = 1.67 (m)	ELA2 AABR = 1.8 (m)	**ELA3 AABR = 1.9 (m)**	ELA4 AABR = 2.0 (m)	ELA5 AAR = 0.5 (m)	ELA6 AAR = 0.6 (m)
All Ben More Coigach glaciers	*1.25*	*331*	*330*	***328 ± 16***	*327*	*325*	*312*
Cadh' a' Mhoraire glacier	0.59	349	347	**345 ± 14**	343	351	326
Sgùrr an Fhidleir glacier	0.30	338	336	**335 ± 13**	334	331	321
An Clù-nead glacier	0.36	307	306	**305 ± 11**	304	294	289

Table 2. Precipitation values and uncertainty for the Ben More Coigach glaciers at the average ELA and at sea level, calculated using the AABR = 1.9 ± 0.81 ELA. The results of both the Ohmura et al. (1992) and Golledge et al. (2010) precipitation-temperature relationships are displayed, where S-type = summer-type precipitation, N-type = neutral-type precipitation and W-type = winter-type precipitation. Palaeoprecipitation values are presented for both a mean July temperature (T_j) at sea level of 8.5 ± 0.3ºC (Benn and Ballantyne, 2005) and a summer sea-level temperature of 6.38ºC (Golledge, 2008).

T_j at sea level (ºC)	Effective precipitation at the ELA (mm a^{-1})				Effective precipitation at sea level (mm a^{-1})			
	Ohmura et al. (1992)	Golledge et al. (2010)			Ohmura et al. (1992)	Golledge et al. (2010)		
		S-type	N-type	W-type		S-type	N-type	W-type
8.5 ± 0.3	2817 ± 425	3204 ± 328	2288 ± 234	1831 ± 187	2343 ± 335	2665 ± 249	1903 ± 178	1523 ± 142
6.38	2065 ± 302	2134 ± 131	1524 ± 101	1219 ± 81	1717 ± 238	1775 ± 102	1268 ± 73	1014 ± 58

Table 3. Potential snowblow areas (expressed as a percentage of the total snowblow area) and snowblow factors for each 90° sector, calculated based on the approaches outlined by Sissons (1980a) and Mitchell (1996).

Glacier	Area (km^2)	Total snowblow area (km^2)	Snowblow area by 90° sectors (percentage of total area)						Snowblow factor by 90° sectors						Total snowblow factor
			NE	SE	SW	NW	S	W	NE	SE	SW	NW	S	W	
Cadh' a' Mhoraire	0.59	3.29	0.0	21.0	76.3	2.7	8.2	75.7	0.00	1.08	2.06	0.39	0.68	2.05	2.36
Sgùrr an Fhidleir	0.30	2.64	0.0	10.6	88.6	1.9	26.9	72.3	0.00	0.95	2.75	0.25	1.51	2.48	2.92
An Clù-nead	0.36	2.88	0.0	2.1	87.8	10.1	57.3	42.0	0.00	0.41	2.65	0.90	2.14	1.83	2.83

Table 4. Potential avalanche areas (expressed as a percentage of the total avalanche area) and avalanche factors for each 90° sector.

Glacier	Area (m^2)	Total avalanche area (m^2)	Avalanche area by 90° sectors (percentage of total area)						Avalanche factor by 90° sectors						Total avalanche factor
			NE	SE	SW	NW	S	W	NE	SE	SW	NW	S	W	
Cadh' a' Mhoraire	588,005	109,837	0	39.9	60.1	0.0	51.1	36.3	0	0.07	0.11	0.00	0.10	0.07	0.19
Sgùrr an Fhidleir	303,137	61,607	0	5.1	58.4	35.7	20.6	78.5	0	0.01	0.12	0.07	0.04	0.16	0.20
An Clù-nead	358,871	118,807	0	43.8	55.4	7.2	64.8	32.2	0	0.14	0.18	0.02	0.21	0.11	0.33

Table 5. Comparison of sea-level equivalent annual precipitation values for Ben More Coigach, the West Sutherland icefield (Lukas and Bradwell, 2010) and the Beinn Dearg ice-cap (Finlayson et al., 2011), with the sites arranged south to north. The precipitation values for West Sutherland and Beinn Dearg were recalculated by Boston et al. (2015) using the approaches outlined in the text (see *'Palaeoclimatic reconstruction'*). ELAs based on AABR = 1.8 have been used for direct comparison, as the earlier studies did not employ AABR = 1.9 ± 0.81.

Ice mass(es)	Reference	ELA	ELA method	Effective precipitation at sea level (mm a^{-1})			
				Ohmura et al. (1992)	Golledge et al. (2010)		
					S-type	N-type	W-type
Beinn Dearg	Finlayson et al. (2011)	576	AABR 1.8	1562 ± 360	1639 ± 425	1171 ± 361	937 ± 329
Ben More Coigach	This study	330	AABR 1.8	2336 ± 320	2655 ± 225	1897 ± 161	1517 ± 129
West Sutherland	Lukas and Bradwell (2010)	339	AABR 1.8	2283 ± 356	2582 ± 427	1844 ± 362	1475 ± 330

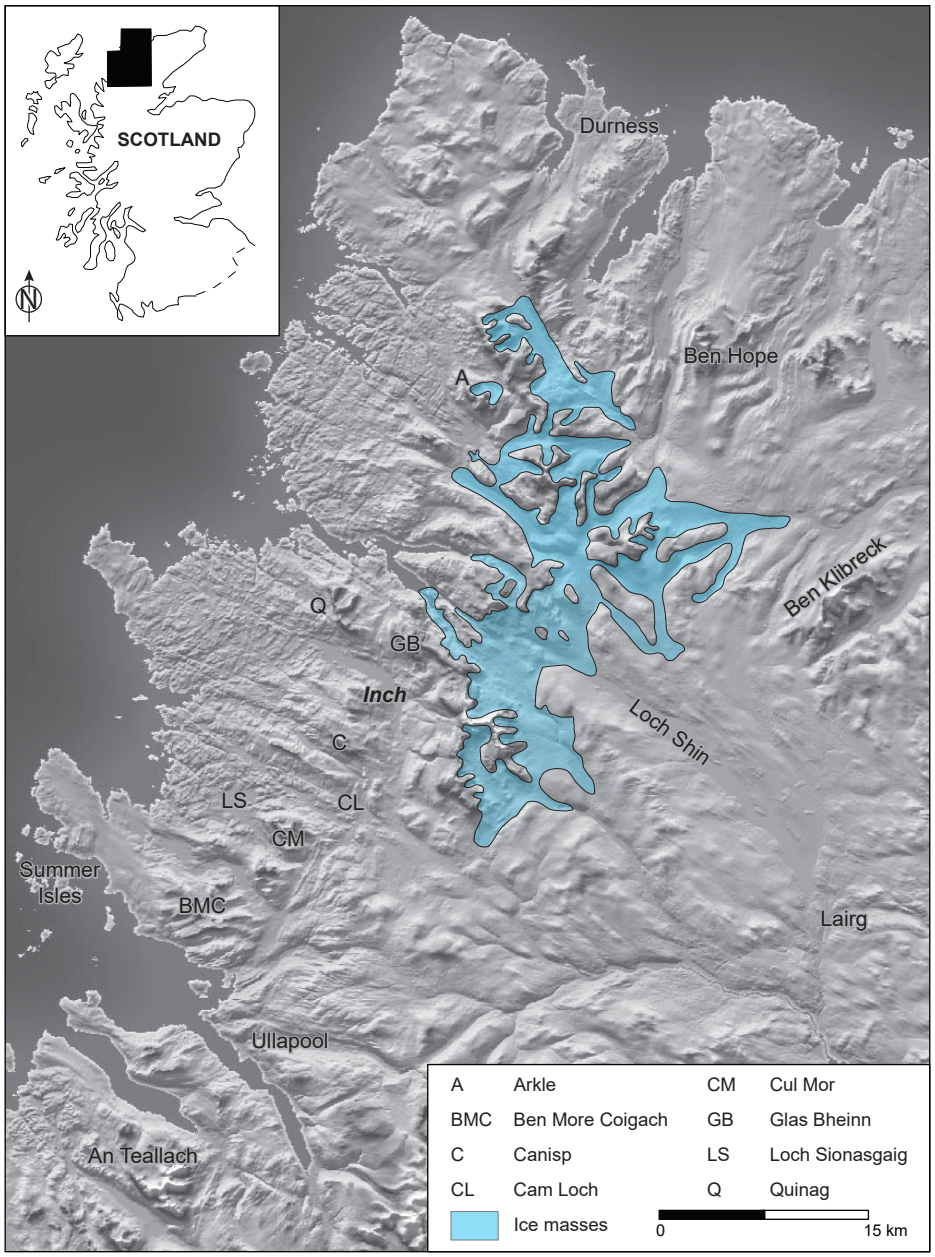
SCOTLAND
Durness
Ben Hope
A
Ben Klibreck
Q
GB
Inch
Loch Shin
C
LS
CL
CM
Summer Isles
BMC
Lairg
Ullapool
An Teallach
A Arkle
BMC Ben More Coigach
C Canisp
CL Cam Loch
Ice masses
CM Cul Mor
GB Glas Bheinn
LS Loch Sionasgaig
Q Quinag
0
15 km

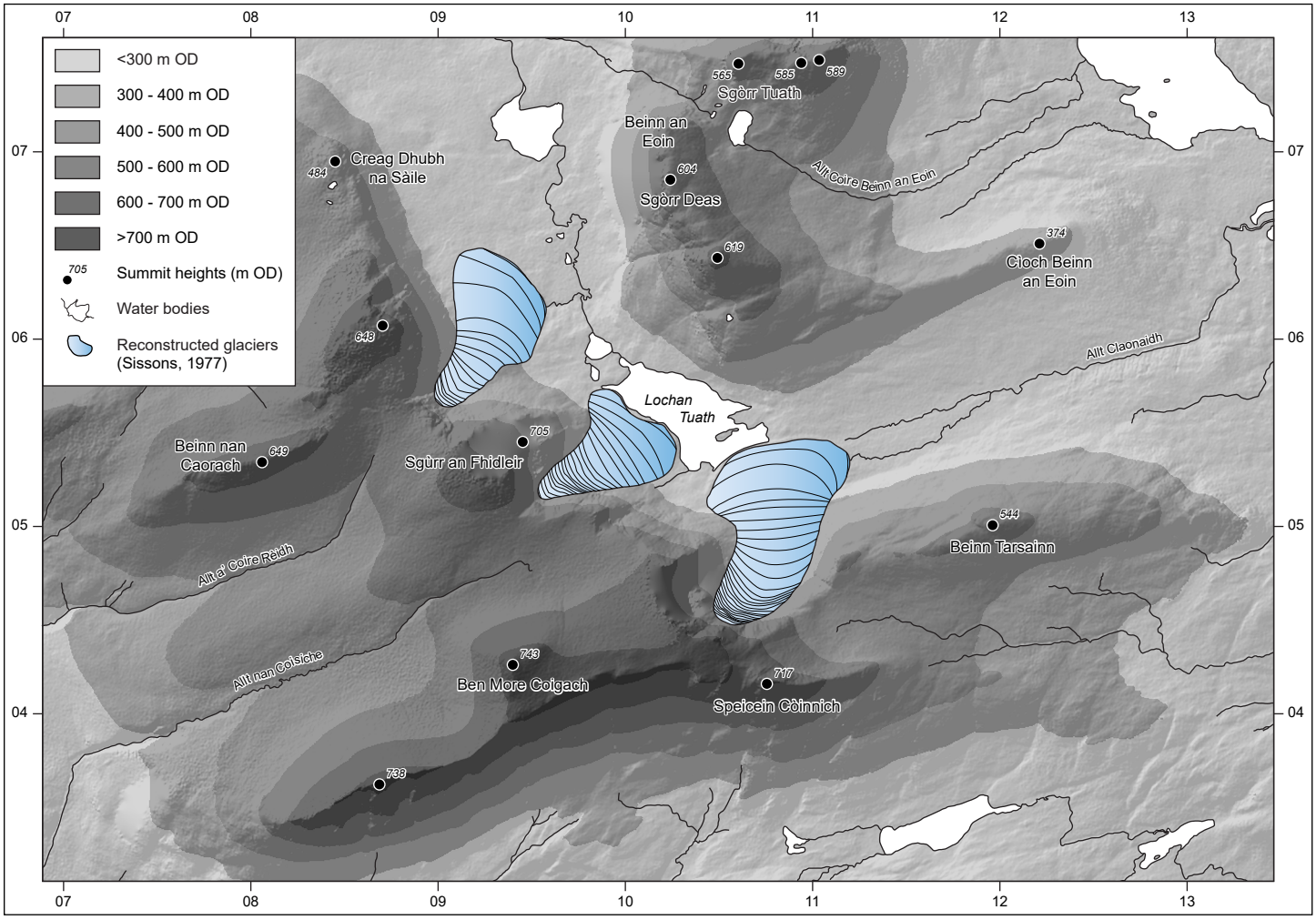
<300 m OD
300 - 400 m OD
400 - 500 m OD
500 - 600 m OD
600 - 700 m OD
>700 m OD
705 Summit heights (m OD)
Water bodies
Reconstructed glaciers (Sissons, 1977)
07
08
09
10
11
12
13
04
05
06
Sgòrr Tuath
565
585
589
Beinn an Eoin
Creag Dhubh na Sàile
484
Sgòrr Deas
604
Allt Coire Beinn an Eoin
619
374
Cìoch Beinn an Eoin
648
Allt Claonaidh
Lochan Tuath
Beinn nan Caorach
649
Sgùrr an Fhidleir
705
544
Beinn Tarsainn
Allt a' Coire Reidh
Allt nan Coisiche
749
Ben More Coigach
717
Speicein Còinnich
738

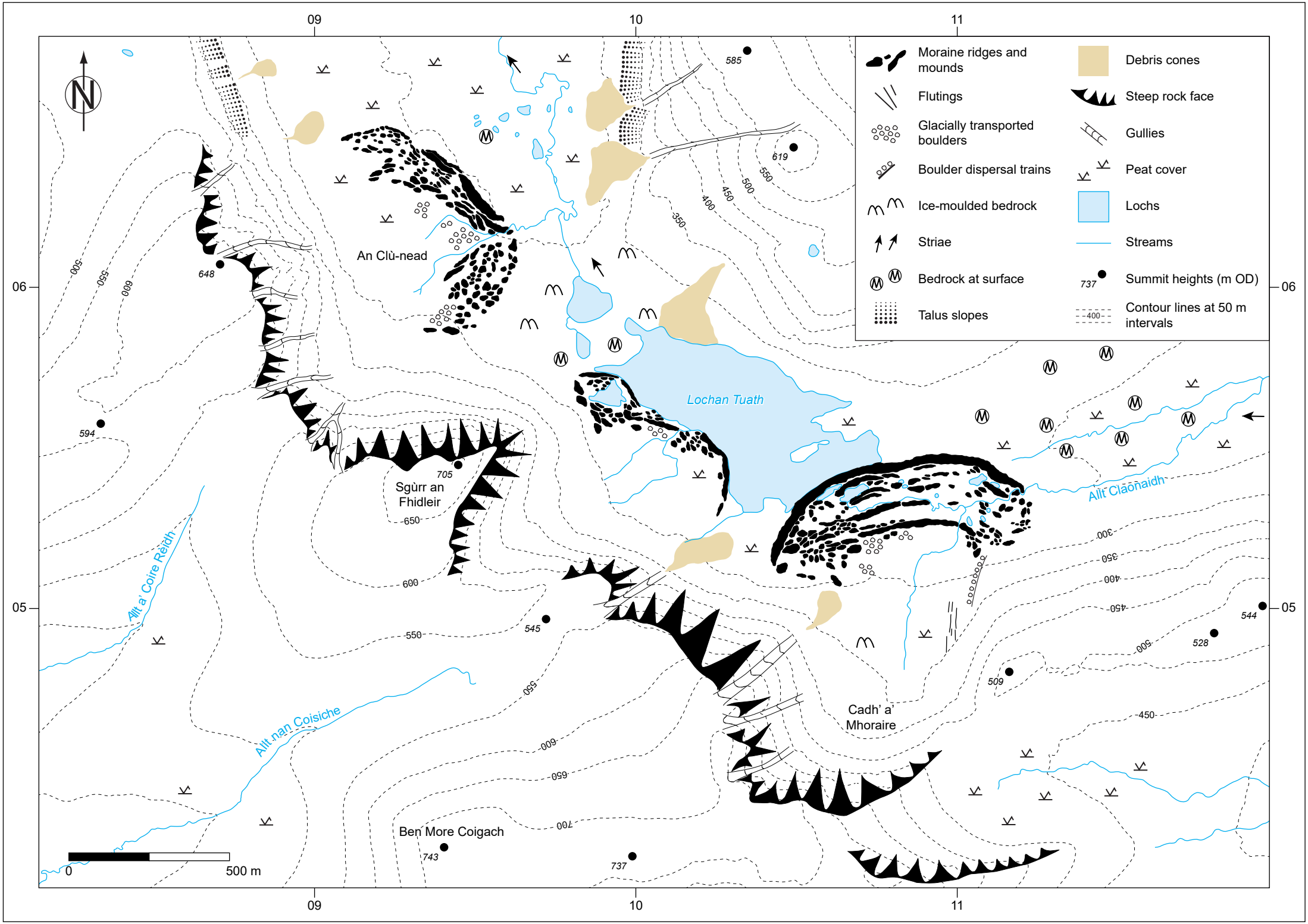
09
10
11
06
05
N
Moraine ridges and mounds
Flutings
Glacially transported boulders
Boulder dispersal trains
Ice-moulded bedrock
Striae
Bedrock at surface
Talus slopes
Debris cones
Steep rock face
Gullies
Peat cover
Lochs
Streams
737 Summit heights (m OD)
400 Contour lines at 50 m intervals
An Clù-nead
Lochan Tuath
Sgùrr an Fhidleir
Allt a' Coire Rèidh
Allt nan Coisiche
Allt Claonaidh
Cadh' a' Mhoraire
Ben More Coigach
585
619
648
594
705
545
509
544
528
743
737
0
500 m

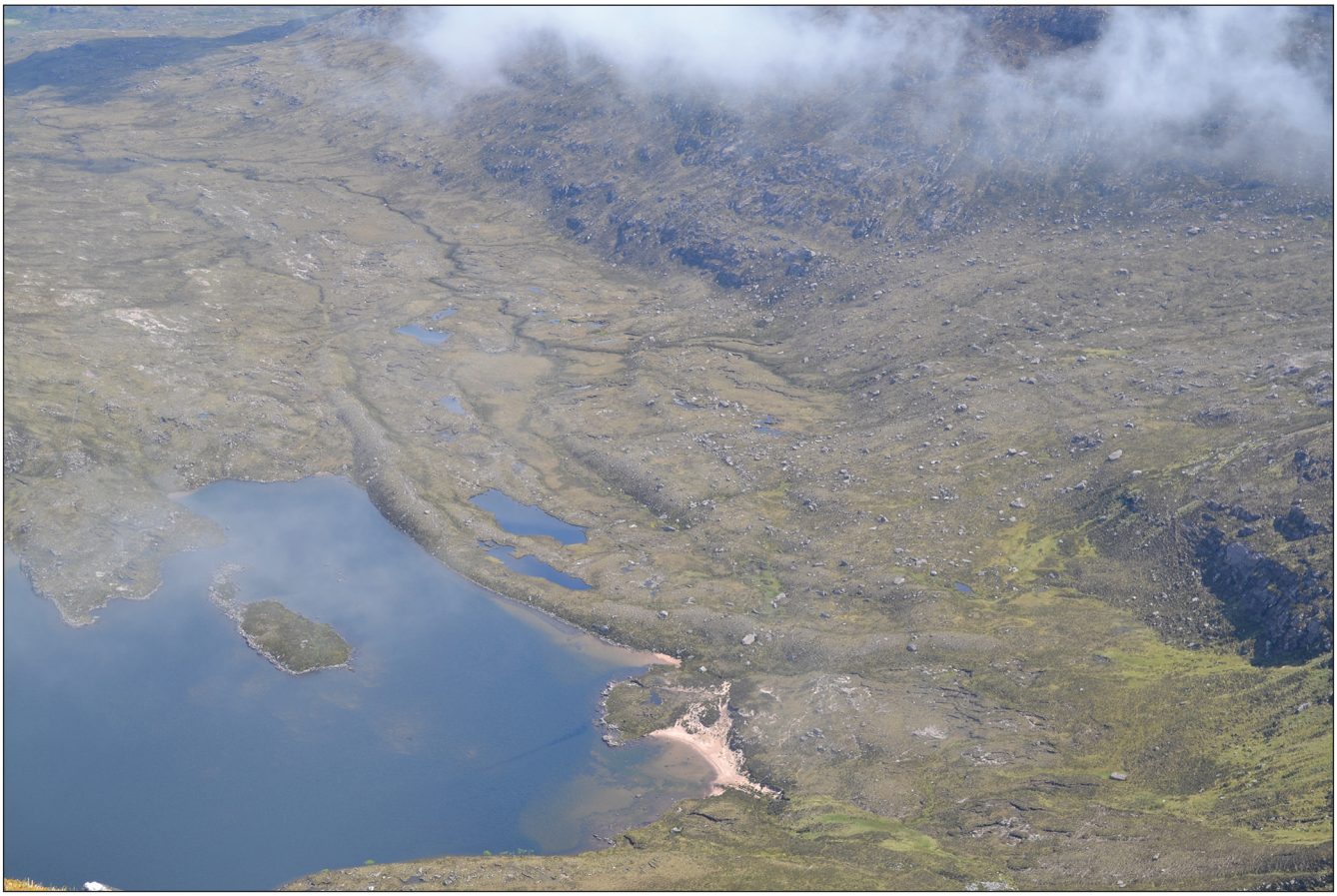


A


C


B


D

Cadh' a' Mhoraire

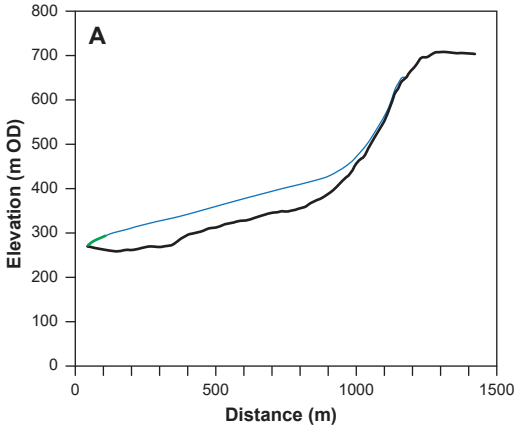

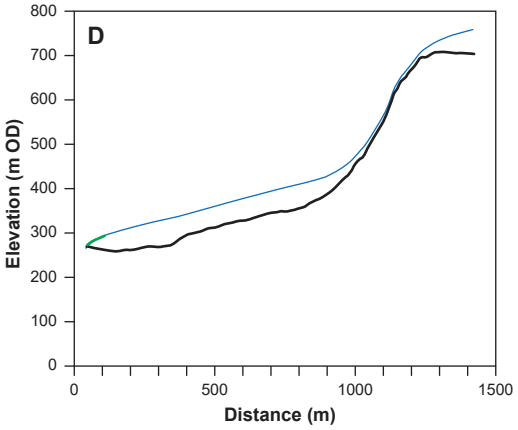

Sgùrr an Fhidleir

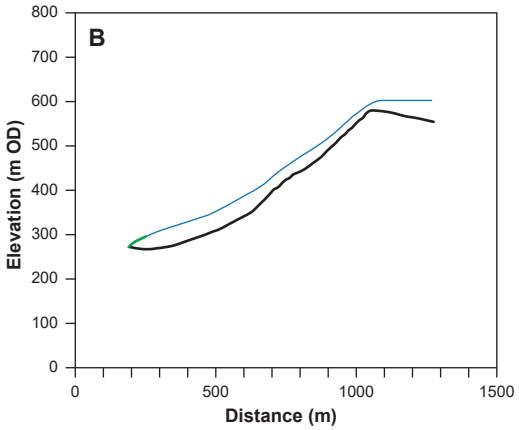

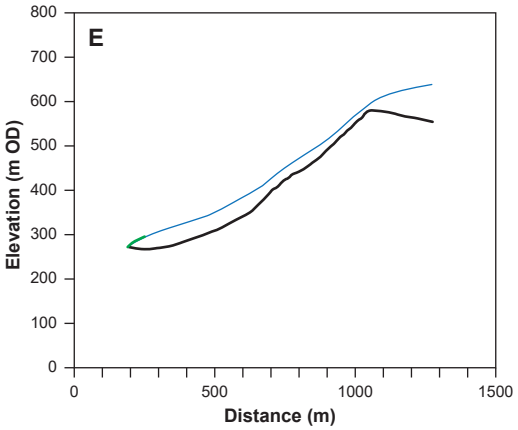

An Clù-nead

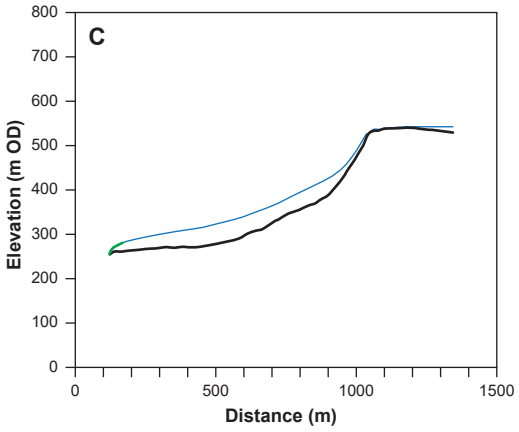

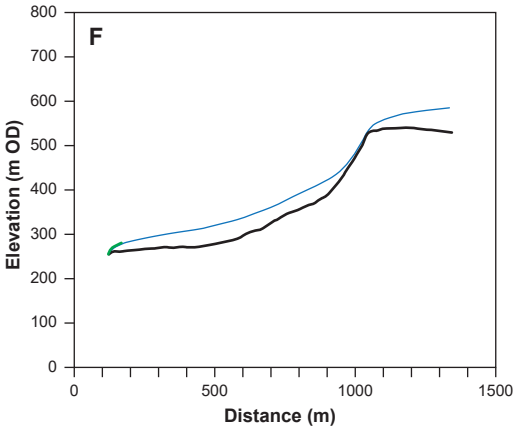

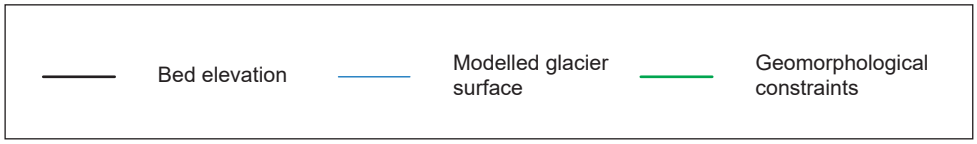

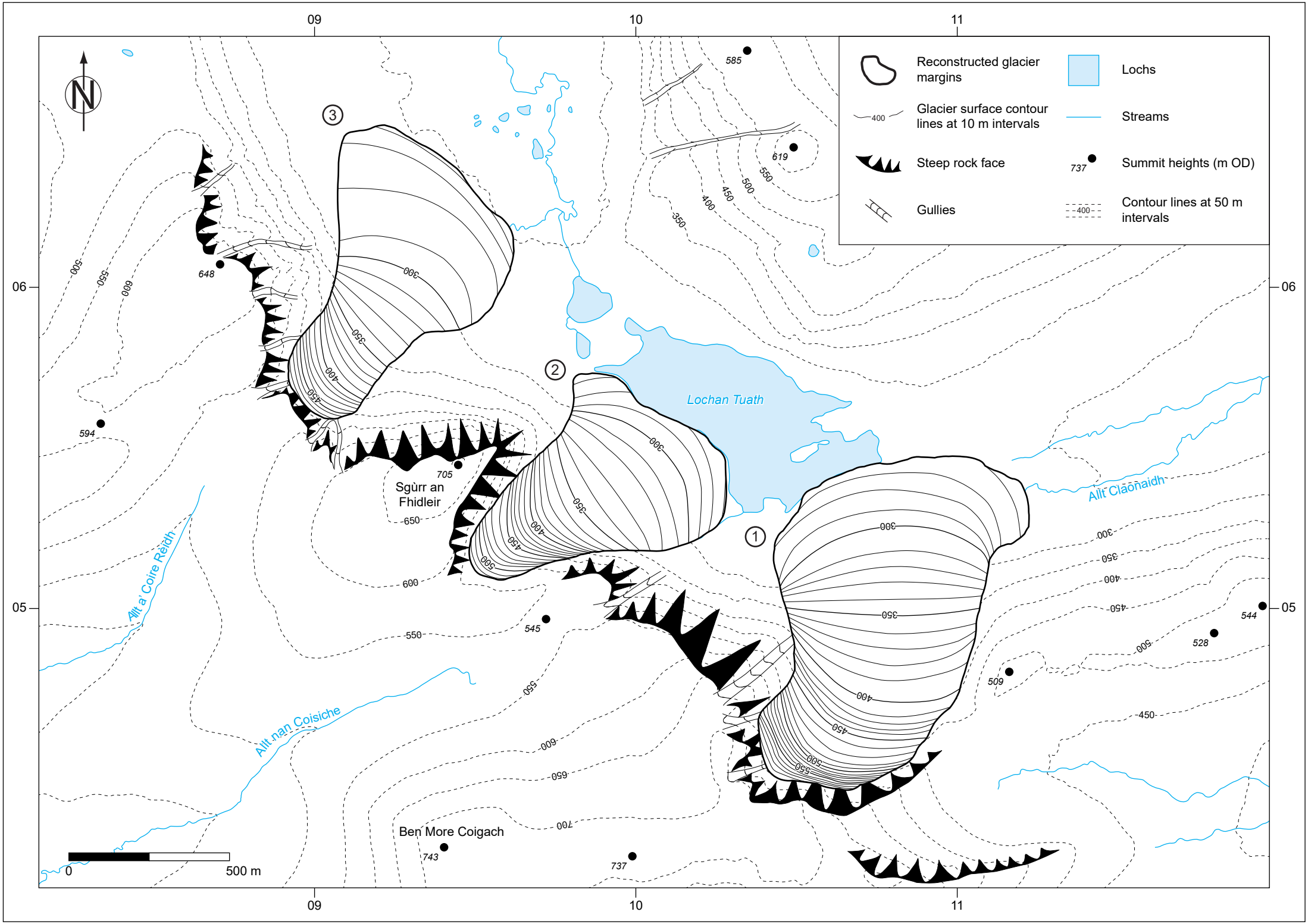
09
10
11
06
05
N
Reconstructed glacier margins
Lochs
Glacier surface contour lines at 10 m intervals
Streams
Steep rock face
Summit heights (m OD)
Gullies
Contour lines at 50 m intervals
1
2
3
Lochan Tuath
Sgùrr an Fhidleir
Ben More Coigach
Allt a' Coire Rèidh
Allt nan Coisiche
Allt Claonaidh
585
619
648
594
705
545
544
528
509
743
737
0
500 m

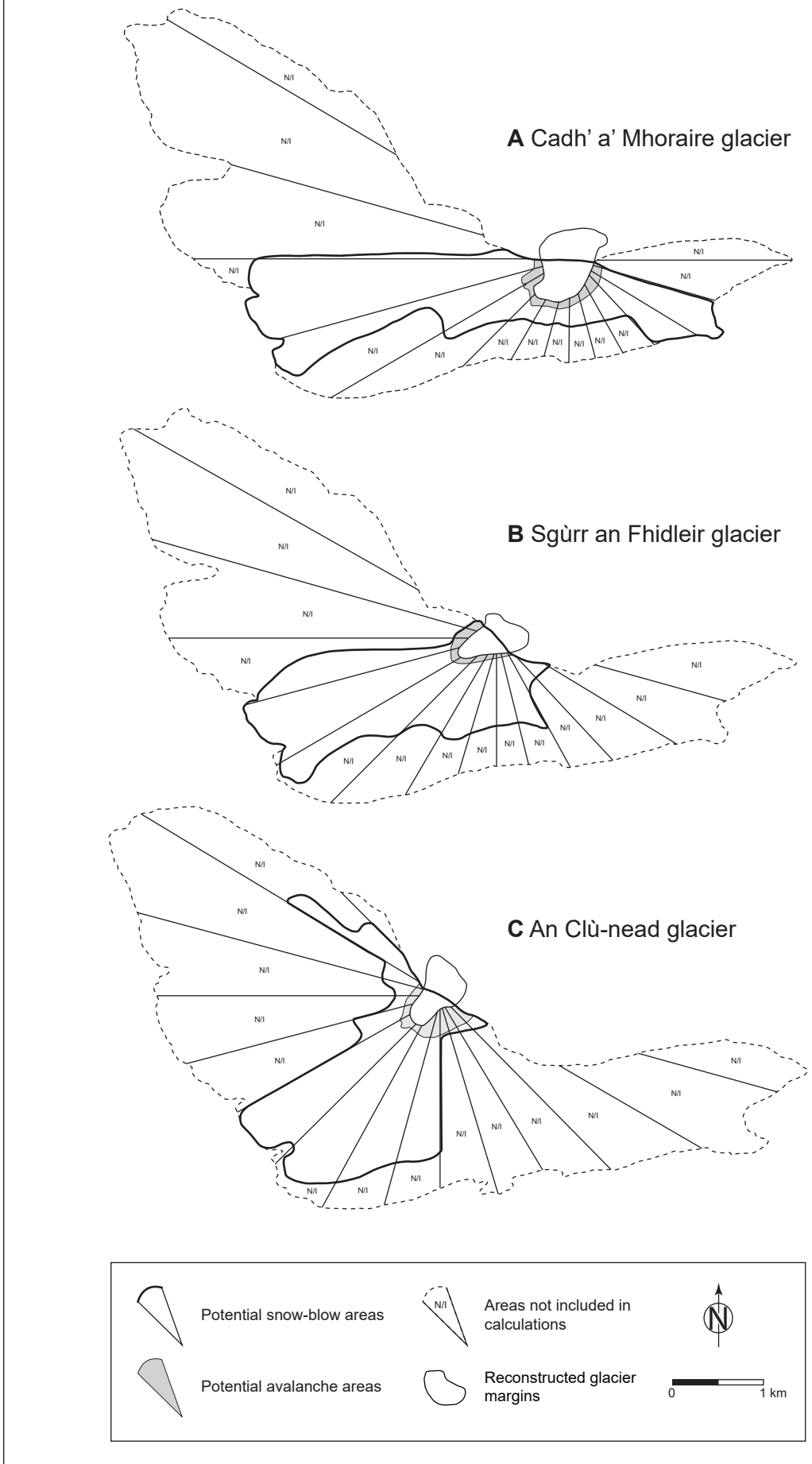
A Cadh' a' Mhoraire glacier
B Sgùrr an Fhidleir glacier
C An Clù-nead glacier
N/I
Potential snow-blow areas
Potential avalanche areas
Areas not included in calculations
Reconstructed glacier margins
N
0
1 km